2015

DEPARTAMENTO DE CIÊNCIAS DA VIDA

FACULDADE DE CIÊNCIAS E TECNOLOGIA
UNIVERSIDADE DE COIMBRA

Unloading driven Cardiac Regeneration: CITED4 in control

Andreia Pinheiro Vilaça

2015

Unloading driven Cardiac Regeneration: CITED4 in control

Andreia Pinheiro Vilaça

DEPARTAMENTO DE CIÊNCIAS DA VIDA

FACULDADE DE CIÊNCIAS E TECNOLOGIA
UNIVERSIDADE DE COIMBRA

Unloading driven Cardiac Regeneration: CITED4 in control

Dissertação apresentada à Universidade de Coimbra para cumprimento dos requisitos necessários à obtenção do grau de Mestre em Biologia Celular e Molecular, realizada sob a orientação do Doutor Hamid el Azzouzi (University Medical Center Utrecht) e do Professor Doutor Carlos Jorge A. M. Bandeira Duarte (Universidade de Coimbra)

Andreia Pinheiro Vilaça

2015

University Medical Center
Utrecht

All experimental activities were performed at the Experimental Cardiology Lab at the University Medical Center Utrecht, the Netherlands.

Utrecht, 2015

Acknowledgments

More than the last year of the Master and the year to write a thesis, this year was a year of great challenges, not only at work but also at a personal level. Moving abroad is not easy and working within a different culture is even more challenging. This work would not be possible without the help of several people, to whom I would like to express my full gratitude.

In the first place, I would like to thank Joost Sluijter for accepting me to work at the experimental cardiology lab and provide me an excellent learning opportunity and work environment.

Moreover, I would like to thank my supervisor and friend, Hamid el Azzouzi for accepting me on his project, for making me feel at home and for always providing a stimulating learning environment. Thanks for trusting me and for encouraging me as a scientist: I really needed someone to boost me in this internship and to “schnizel me” with passion for science. I will never forget the late hours at the GDL and the long FL talks behind the microscope. You made me believe it is possible to have fun at work while doing great science. Thanks for all the fun and crazy work this year, you are awesome!

I would also like to thank everyone from the experimental cardiology lab for all the help and nice times in the lab.

Ao nível de trabalho, gostaria ainda de agradecer ao professor Carlos Duarte e à professora Emília Duarte, pela dedicação ao mestrado e empenho na excelência do mesmo e pela ajuda e apoio inicial para esta tese.

Living within a different culture is not always easy but some people make me enjoy the most of it and deserve my complete gratitude for that. In this regard I would like to thank Benjamin, Mio, Lena, Nathan and specially Corianne. Although in different aspects, all of you contributed for a very nice stay in Utrecht and made me enjoy the most of it, overcoming all the difficulties.

Gostaria ainda de agradecer aos meus amigos portugueses que apesar da distância, estiveram sempre perto e foram um suporte para mim neste ano de desafios. Assim, agradeço especialmente à Maria, ao Rui e à Rita pelo companheirismo e carinho que ajudaram a ultrapassar os maiores obstáculos.

Por último, mas não menos importante, gostaria de agradecer aos meus pais por todo o apoio e força que sempre me deram para seguir os meus sonhos e por toda a paciência que sempre tiveram nos momentos mais difíceis. Obrigada pela educação que sempre me deram que me transformou na pessoa que sou hoje. Por tudo isto e muito mais, o meu muito obrigado!

Abstract

Despite all the years of intense research on heart failure, it is still the number one cause of death worldwide, and thus, finding new therapeutical target possibilities to develop a treatment is vital. The discovery of stem cells in the adult heart and the fact that cardiomyocyte renewal was shown to occur throughout life contradict the long standing belief that the heart is a post mitotic organ. However, upon injury the heart is not able to regenerate itself and administration of exogenous stem cells show controversial results without relevant neomyogenesis. Thus, unravelling the mechanisms that drive endogenous cardiac regeneration may be a powerful tool to provide rationale on how this process is regulated and what strategies might be used to enhance myocardial regeneration after injury.

Upon injury the heart responds to a variety of biochemical and hemodynamic stressors through adverse cardiac remodeling which is comprised of pathological hypertrophy, fibrosis and tissue loss. This response induces DNA duplication and nuclear division followed by cell cycle arrest, contrary to what happens in physiological hypertrophy where cardiomyocyte renewal is maintained or enhanced which was associated with increased levels of CREB-binding protein (CBP)/p300-interacting transactivator with ED-rich carboxy-terminal domain 4 (CITED4).

Left ventricular assist devices relieve the pressure overload from the heart and promote great functional recovery to heart failure patients including reversal of chamber enlargement, fibrosis and stress markers.

In this work we developed a unique unloading mice model to study endogenous cardiac regeneration after TAC induced pressure overload. Vehicle or tamoxifen treated α-MHC-MCM-CITED4$^{f/f}$ were used to investigate the cardiac specific role of CITED4 in the unloading induced regeneration. We demonstrate that lack of CITED4 in the heart hampers fast cardiac regeneration in response to unloading that is accompanied by persistence of fibrosis and elevated stress marker expression. Moreover, we provide evidence that mitosis of cardiomyocytes takes part in the recovery process upon unloading and that cardiac CITED4 is essential herein.

Key Words: cardiac unload, endogenous cardiac regeneration, cardiac remodeling, cardiomyocyte renewal, CITED4

Resumo

Apesar de intensa investigação em falência cardíaca, esta continua a ser a causa número um de morte no Mundo, e portanto, é vital descobrir novos alvos terapêuticos para desenvolvimento de uma terapia. A descoberta de células estaminais no coração adulto e o facto da renovação de cardiomiócitos ao longo da vida ter sido demonstrada contraria a natureza pós-mitótica do coração em que se acreditava. No entanto, após danos no coração, este não é capaz de se regenerar e a administração de células estaminais exógenas tem demonstrado efeitos controversos sem neomiogénese relevante. Desta forma, entender os mecanismos endógenos que promovem regeneração cardíaca poderá ser importante para perceber como este processo é regulado e que estratégias adotar para tornar a regeneração do miocárdio mais eficiente após patologias cardíacas.

Patologias cardíacas induzem uma resposta de remodelação cardíaca adversa que consiste em hipertrofia patológica, fibrose e morte celular. Esta resposta promove duplicação do DNA e divisão nuclear seguida de paragem do ciclo celular, contrariamente ao que acontece em condições de hipertrofia fisiológica em que a renovação de cardiomiócitos é mantida ou melhorada associada ao aumento dos níveis de CREB-binding protein (CBP)/p300-interacting transactivator with ED-rich carboxy-terminal domain 4 (CITED4).

Dispositivos de assistência ventricular esquerda aliviam a pressão no coração e promovem uma grande recuperação funcional em pacientes com falência incluindo regressão do alargamento das câmaras cardíacas, de fibrose e dos marcadores de stress.

Neste trabalho desenvolvemos um modelo animal único composto por alterações hemodinâmicas no coração com o objetivo de estudar a regeneração cardíaca endógena. Ratinhos α-MHC-MCM-CITED4$^{f/f}$ tratados com veículo ou tamoxifen foram usados para investigar a função específica de CITED4 na regeneração induzida pela redução de pressão no coração. Aqui demonstramos que a falta de CITED4 no coração dificulta a rápida resposta de regeneração que é, então, acompanhada por persistência de fibrose e elevada expressão de marcadores de stress. Adicionalmente, evidenciamos que mitose de cardiomiócitos está envolvida na recuperação promovida pelo modelo e que CITED4 desempenha um papel essencial neste processo.

Palavras-chave: alívio de pressão cardíaca, regeneração cardíaca endógena, remodelação cardíaca, renovação de cardiomiócitos, CITED4

Abbreviations

α–SMA. α-smooth muscle actin

Akt. Protein kinase B

ANF. Atrial natriuretic factor

Ang II. Angiotensin II

BNP. Brain Natriuretic Peptide

BrdU. 5-Bromo-2-Deoxyuridine

C/EBPβ. CCAAT-enhancer binding protein-β

Cdk. Cyclin-dependent kinase

Cdki. Cyclin-dependent kinase inhibitor

CITED4. CREB-binding protein (CBP)/p300-interacting transactivator with ED-rich carboxy-terminal domain 4

ER. Estrogen receptor

ERK. Extracellular signal regulated kinases

ET-1. Extracellular regulated kinase

FGF-2. Fibroblast growth factor 2

FOXO3. Forkhead box protein O3

GH. Growth hormone

GPCR. G_q protein-coupled receptors

GSK3. Glycogen synthase kinase 3

H&E. Hematoxylin and Eosin staining

HF. Heart failure

HIF-1α. Hypoxia inducible factor-1α

IGF-1. Insulin-like growth factor 1

IGF-1R. Insulin-like growth factor 1 receptor

JNK. c-Jun NH2-terminal kinases

LBD. Ligand-binding domain

lncRNA. Long non-coding RNA

LV. Left ventricular

LVADs. Left ventricular assist devices

LVH. Left ventricular hypertrophy

LVVs. LV systolic volume

MAPK. Mitogen-activated protein kinase

MAPKK. Mitogen-activated protein kinase kinase

MAPKKK. Mitogen-activated protein kinase kinase kinase

MCM. MerCreMer

MEF2. Myocyte enhancer factor 2

MHC. Myosin heavy chain

miR. Micro-RNA

mTOR. Mammalian target of rapamycin

NFAT. Nuclear factor of activated T-cells

PFA. Paraformaldehyde

PH3. Phosphohistone H3

PI3K. Phosphoinositide-3 kinase

PIP3. Phosphatidylinositol 3,4,5-trisphosphate

PP2B. Protein phosphatase 2B

Rb. Retinoblastoma

SAPKs. Stress-activated MAPKs

Sca-1. Stem cell antigen 1

TAC. Transverse aortic constriction

TFAP2. Transcription factor AP-2

TGF-β. Transforming growth factor β

VAD. Ventricular assist device

WGA. Wheat germ agglutinin

Table of Contents

I. Introduction

I. Introduction

Heart failure (HF), is a life-threatening condition characterized by structural or functional impairment of ventricular filling or ejections of blood (1), often associated with considerable emotional and socio-economic burden. In fact, according to the World Health Organization, cardiovascular diseases were the leading cause of death in 2012, killing 17.5 million people in that year. Considering the overall rise in ageing of the general population and high prevalence of risk factors as well as improved survival from cardiovascular events, it is expected that the incidence of heart failure will increase with time along with the direct medical costs associated to it.

Adverse Cardiac Remodeling

Upon injury, the heart responds to a variety of biochemical and hemodynamic stressors through a process called cardiac remodeling which involves molecular, cellular and interstitial alterations that are reflected further in size, shape and function of the heart (2). The initial response is adaptive and tries to keep up with the decline in the pumping capacity of the heart. However, prolonged stress stimulation progressively contributes to deteriorate ventricular function and cause a decompensated dysfunction (3), leading ultimately to heart failure (FIGURE 1). Mechanisms that underlie cardiac remodeling are not yet fully understood, however, three hallmarks are generally considered important for pathological cardiac remodeling: hypertrophy, fibrosis and cell death.

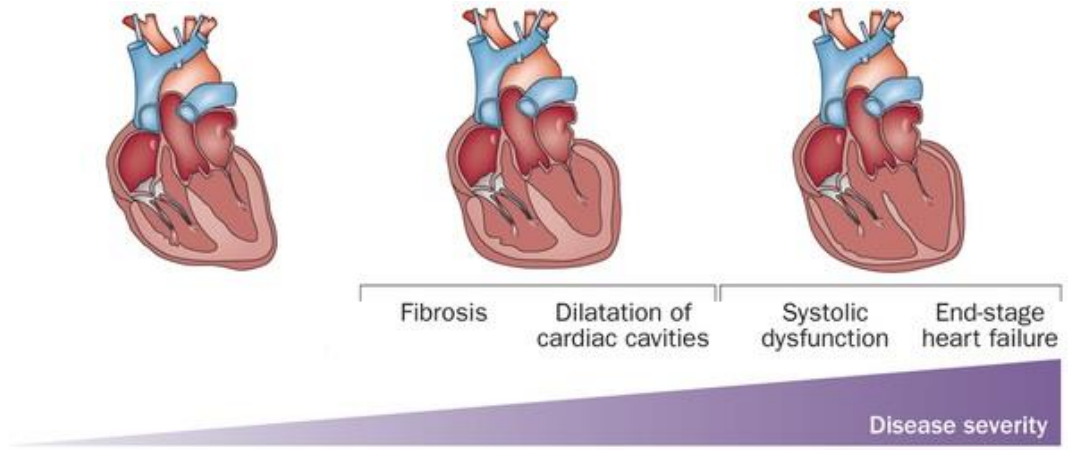

FIGURE 1 | Normal Progression of Heart Failure includes adverse cardiac remodeling. Prolonged stress stimuli on the heart induces adverse remodeling that is initially characterized by hypertrophy, fibrosis and cardiomyocyte loss. Overtime this response is deleterious inducing dilatation of the cardiac cavities further leading to systolic dysfunction. Adapted from Finsterer J and Cripe L, 2014 (4).

Pathological Hypertrophy

Pathological hypertrophy happens when stress stimuli are maintained for a long time. Under these conditions, pathological remodeling of the heart is induced which is characterized by enlargement of existing cardiomyocytes to cope with augmented demand on the heart (5–8).

During mechanical stress, cardiomyocytes secrete angiotensin II (Ang II) and extracellular regulated kinase (ET-1) (8) in response to various neural-humoral agonists/effectors. These molecules bind to Gq protein-coupled receptors (GPCR) promoting its activation (8) and the subsequent activation of downstream effectors. Calcineurin and MAP kinases like extracellular signal regulated kinases 1 and 2 (ERK1/2)(6) are the most thoroughly studied effectors (FIGURE 2).

Calcium-calmodulin-activated protein phosphatase 2B (PP2B), also called calcineurin (9) is a serine/threonine phosphatase that is specifically activated when there is a persistent increase in intracellular calcium [Ca2+] levels (8). In the presence of such stimuli, calmodulin (calcium binding protein) gets saturated and promotes the activation of calcineurin. Once activated, calcineurin is responsible for the direct dephosphorylation of members of the nuclear factor of activated T-cells (NFAT) transcription factor family located in the cytoplasm. This, induces NFAT translocation to the nucleus (8) where it, in coordination with other transcription factors such as GATA4 and myocyte enhancer factor 2 (MEF2), regulate expression of several cardiac hypertrophy related genes including skeletal α actin and brain natriuretic peptide (BNP)(10, 11).

Accordingly, Wilkins and colleagues (12) showed that calcineurin/NFAT signaling was a key enzyme involved in pathological but not physiological hypertrophy of the heart since NFAT activity was upregulated in mouse models of pathological cardiac hypertrophy induced by pressure overload or following myocardial infarction. On the other hand, the same study failed to show significant calcineurin/NFAT coupling in the heart in physiological hypertrophy induced by two different exercise models. Additionally, calcineurin inhibition was proved to prevent the development of cardiac hypertrophy in rodent models of cardiomyopathy and pressure-overload induced hypertrophy (13).

Mitogen-activated protein kinase (MAPK) signaling in the heart has also been implicated to have a role in promoting cardiac hypertrophy. Briefly, stress stimulus from the cells activate MAPK kinase kinase (MAPKKK) which, in turn activate a MAPK kinase MAPKK) through three-tiered sequential phosphorylation events. MAPKK subsequently activates the MAPK through serial phosphorylation.

MAPK subfamilies include ERK1/2, c-Jun NH2-terminal kinases (JNK1, -2 and -3), p38 kinase (α, β, γ, δ), and BMK or ERK5 which have different roles in the cell. Growth factors exert the main stimulation type of ERK 1/2 pathway whereas JNK and p38 [collectively called stress-activated MAPKs (SAPKs)] are mainly induced by stress agents. The ERK5/BMK pathway has been associated with both growth and stress stimuli (14).

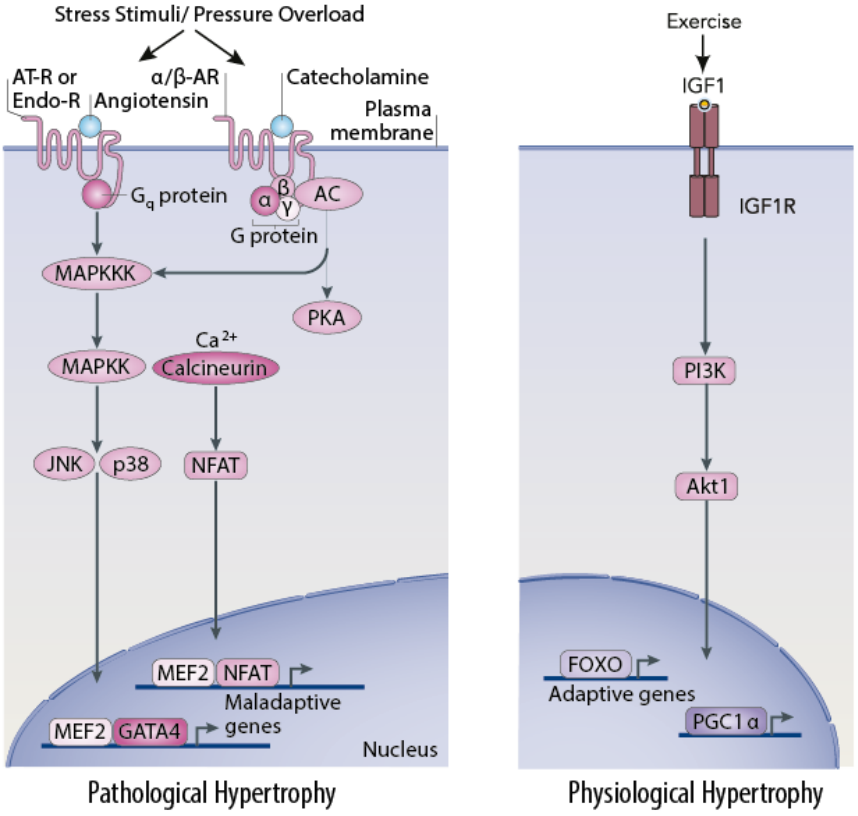

FIGURE 2 | Brief schematic representation on the main described signaling pathways underlying pathological and physiological forms of hypertrophy. On the left panel, angiotensin II (AT), endothelin I (endo) activate G proteins by binding to the receptors they are coupled to. Intracellular Ca^{2+} release is induced which activates calcineurin that further dephosphorylates nuclear factor of activated T cells (NFAT family members) promoting its nuclear translocation. NFAT complexes with the cofactors GATA4 or myocyte enhancer factor-2 (MEF2) to transactivate the transcription of typically maladaptive hypertrophic genes. Pathological cardiac hypertrophy is also mediated by p38 and c-Jun N-terminal kinase (JNK) branches of the MAPK cascade which phosphorylate and activate GATA4. On the right panel, insulin-like growth factor 1 (IGF-1) pathway, which is the most well described signaling cascade that promotes physiological hypertrophy is depicted. Upon exercise, IGF-1 is released and binds to IGF-1 receptor (IGF-1R), inducing its activation. Two downstream effectors that are important for physiological cardiac growth are phosphoinositide 3-kinase p110 α [PI3K(p110 α)] and Akt1. This signaling pathway induces the transcription of adaptive hypertrophy genes promoting protein synthesis and cell survival, eventually enhancing heart function. Adapted from Maillet M et al. 2013 (15).

Next to a change in myocyte phenotype, the hypertrophic response of the stressed adult heart is accompanied by fetal gene programme reactivation including atrial natriuretic factor (ANF), BNP, skeletal α-actin and β-myosin heavy chain (β-MHC)(16). The reactivation of fetal genes seems to be a beneficial adaptive response to increased workload, since for example the fetal isoform of MHC (β -MHC) is bio-energetically more efficient than that of the adult (α-MHC), since its slower at catalyzing hydrolysis of ATP(16). However, on the long term, these quantitative changes in the composition of the contractile apparatus of the stressed heart are associated with depressed contractility and heart failure (16). Another part of the return to a fetal programme is the fact that the failing heart also exhibits a metabolic pattern that is hallmarked by impaired mitochondrial fatty acid oxidation and a shift to further reliance on glucose metabolism (15). Due to the lowered consumption and the subsequent accumulation of fatty acids, increased synthesis of uncoupling proteins and the deterioration of the electrochemical gradient across the inner mitochondrial membrane, hampers mitochondrial activity causing reduced ATP production and diminished cardiac function (17).

Fibrosis and Cardiomyocyte loss

In the adult mammalian myocardium, fibroblasts are the most abundant interstitial cells (18, 19). They are the major producers of extracellular matrix proteins and are thus responsible for keeping cardiac matrix integrity contributing to preservation of cardiac geometry (20).

Following myocardial injury, fibroblasts are activated and participate in cardiac remodeling. Associated with intense angiogenesis, fibroblasts and endothelial cells infiltration of the damaged area (21, 22). During this phase, fibroblasts are activated by transforming growth factor β (TGF-β) and transdifferentiate into myofibroblasts (21). Cardiac Myofibroblasts, expressing α-smooth muscle actin (α–SMA) and other contractile proteins (22), synthesize and release matrix protein needed for maintenance of the structural integrity of the myocardium (19). In this phase cellular proliferation ceases and matrix is used to fill the damaged area ultimately leading to the establishment of a dense collagen-based scar that results from matrix cross-linking mostly referred to as replacement fibrosis (23). This is mostly perivascular around intramyocardial blood vessel and in areas of extensive cardiomyocyte death (24). Cardiomyocyte loss is a major contributor to the later phase of cardiac remodeling and there is clinical and pathological evidence for all the three well described death mechanisms (25). In

fact, upon sustained stress, cardiomyocytes lose sarcomeric organization and increase cytoskeletal elements which leads to progressive ventricular dilatation, characterized by ventricular enlargement and wall thinning (26). Enlargement of the ventricle not proportionally to wall thickness is responsible for increased wall stress that further stimulates already overloaded myocyte region triggering cell death (27).

Physiological Hypertrophy

Physiological hypertrophy is known for driving the growth of the heart from birth to early adulthood as well as during pregnancy or repetitive exercise (15). Physiological remodeling differs in its structural and molecular profile from pathological hypertrophy. Contrary to the latter, it maintains or enhances cardiac function through development of bigger and better sarcomeric structure that is reflected on increased heart size (28) without signs of fibrosis or cell death (16).The most well-known signaling pathway that regulates physiological cardiac hypertrophy is that which is initiated by insulin-like growth factor 1 (IGF-1). In response to systemic growth hormone (GH), IGF-1 is produced and secreted by the liver and then targeted to the different tissues to promote growth. In addition, target tissues can also produce IGF-1 (15). Upon exercise induced hypertrophic stimuli, IGF-1 levels increase and bind to IGF-1 Receptor (IGF-1R) promoting its activation (6). Once activated, it directly stimulates phosphoinositide-3 kinase (PI3K) (5, 6), that further leads to the phosphorylation and activation of protein kinase B (Akt) through phosphatidylinositol 3,4,5-trisphosphate (PIP_3) (6, 29, 30). In fact, PI3K is vital not only for inducing physiological hypertrophy but also to protect the heart against pathological stimuli (6). Miyamoto and colleagues showed that PI3K-Akt pathway was proved to be crucial in the determination of heart size since activation of Akt was predominant in volume-overloaded hearts (29). The heart also express both isoforms of glycogen synthase kinase 3 (GSK3), GSK3α and GSK3β, that are inhibited by the action of Akt and further promote cardiac hypertrophy (16). Akt is also responsible for increased protein translation through Inhibition of GSK3β and activation of mammalian target of rapamycin (mTOR). Moreover, Akt induces overall reduced protein turnover and catabolism through the inhibition of the activity of forkhead box protein O3 (FOXO3), favoring the net protein accumulation needed for hypertrophy (15).

Furthermore, contrary to pathological hypertrophy, physiological hypertrophy has been associated with maintenance or improved cardiomyocyte renewal, both through the differentiation and further proliferation of stem cells and

the cycling of pre-existing cardiomyocytes. Mechanisms involved in physiological hypertrophy provide a good environment for hyperplasia of cardiomyocytes and activation of stem cells as seen during endurance exercise (31–33). Although increased proliferation markers have been reported in the border zone of an infarct area in Humans, regeneration of the heart post injury is not significant (34–36). Therefore it might be postulated that these cardiomyocytes underwent nuclear duplication, without complete cell division (37). Hence it is believed that unlike pathological hypertrophy, physiological hypertrophy (in which a clear benefit in function is seen), myocytes can undergo cytokinesis and complete the cell cycle, contributing to new myocyte formation.

Mechanistically, activation of IGF-1 pathway was shown to stimulate myocyte proliferation both in culture of newborn rat isolated cardiomyocytes (38) and in mice overexpressing IGF-1 in the heart (39). Moreover, IGF-1 inhibition in isolated cardiomyocytes led to a decrease in growth, nuclear mitosis and DNA synthesis (38). Overall, downstream signaling of IGF-1 seems to play a role in the delicate balance between cardiomyocyte division and hypertrophy. Akt was shown to promote cardiomyocyte hypertrophy when overexpressed at non-physiological levels (40) while its physiological translocation to the nucleus was implicated in hyperplastic phenotype with increased number of cell division (41). IGF-1 signaling has also been correlated with protection against senescence through the increase in telomerase activity and contribution for the maintenance of the cardiac stem cell pool (42). In summary, IGF-1 has an important role in cell division and adaptive hypertrophy, possibly being a valuable pathway to manipulate in order to achieve regeneration after injury.

Current Treatment Approaches

Considering the impact of HF worldwide, finding a strategy to restore cardiac function or prevent its decrease is of urgent concern.

Currently, several pharmaceutical drugs and surgical techniques are used to prevent further decline in heart function or to restore the function of a failing heart, with the ultimate goal of prolonging patients' life. Among all treatments available, the ones most widely used include beta-blockers (43, 44), angiotensin converting enzyme inhibitors (45, 46), valve replacement or reconstruction (47, 48) and reperfusion/ revascularization (49). Although, these therapeutic options proved beneficial and substantially decreased mortality rates over the past 30 years, the only treatment available for end-stage heart failure is heart transplantation.

Unfortunately, heart transplantation presents some limitations including reduced organ supply and life-long immune suppression, with a variety of associated complications. Therefore transplantation will not be a complete solution for heart disease problems.

Another avenue for restoring heart function that has recently become more popular is cardiac regeneration research, focusing mostly on stem cell therapies for improvement of endogenous cardiac regeneration.

Stem cell therapies raised attention when in 2003, Beltrami et al. (50) first described the existence of Lin^- $c\text{-}kit^+$ cells in the adult heart. These cells were shown to behave as cardiac stem cells since they were self-renewing, multipotent and clonogenic as well as able to differentiate into myocytes, smooth muscle and endothelial cells (50). Following the discovery of these cells in the heart, other cardiac stem cell like cells were reported such as Stem cell antigen 1 (Sca-1) positive cells, $isl1^+$ cells and side population cells, all of them showing some potential to differentiate into cardiomyocytes (51–54).

Considering the promising capacity of stem cells to differentiate and eventually restore the damaged myocardium upon injury, there was a boost on stem cell research for possible therapy development. In a randomized and blinded clinical trial (REPAIR-AMI), functional improvements and reduction of major adverse cardiovascular events at 2 years post transplantation were observed (55). However, two recent clinical trials show discouraging results upon evaluation of safety and efficacy of bone-marrow-derived cell therapies (56). Other than aiming to understanding the effect of bone marrow-derived cell therapy after myocardial infarction, Timing In Myocardial infarction Evaluation (TIME) trial and the POSEIDON trial have little in common. The first, failed to show any improvement on left ventricular ejection fraction, measure for the ventricular function after intracoronary delivery of autologous bone marrow cells (57). Although the latter trial was able to demonstrate a safety profile, it did also not show significant improvement in ventricular function after transendocardial delivery of bone marrow-derived cells in ischemic cardiomyopathy patients (58). Moreover, skeletal muscle has been shown to efficiently regenerate through satellite cells (progenitor cell pools in skeletal muscle). However, functional integration of skeletal muscle cells in the heart does not occur *in vivo* (MAGIG trial) (59, 60). While progress has been made with increasing number of clinical trials running worldwide, there remain technical and biological hurdles that limit current success of these approaches. For example, no consensus has been achieved regarding the ideal cell type for transplantation, the best method of cell delivery or the mechanisms of potential efficacy. Ultimately,

although clinical trials have shown some efficacy, the therapy still showed poor homing and/or low engraftment of these stem cells in the heart without relevant neomyogenesis (61, 62).

Despite the presence of stem cells in the heart and their contribution to maintain heart function throughout life, upon injury the percentage of cardiomyocytes that are derived from c-kit+ cells is astonishingly low (63). The fact that normal cardiomyocyte proliferation that maintains cardiomyocyte turnover throughout life (64), is insufficient to regenerate the myocardium after injury remains puzzling. It might thus be postulated that relevant neomyogenesis that is sourced either by stem cells or cardiomyocyte cell division is hampered in the failing heart (FIGURE 3). In this light, unravelling the mechanisms that drive endogenous cardiac regeneration might be a powerful tool to provide rationale on how this process is regulated and what strategies might be used to enhance myocardial regeneration after injury (65).

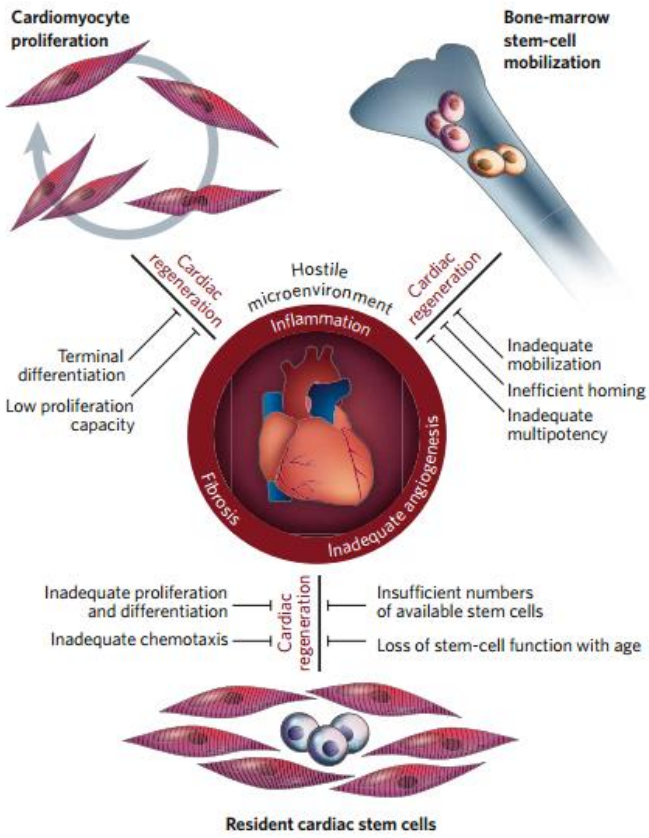

FIGURE 3 | Proposed mechanisms of endogenous cardiac regeneration upon injury and potential barriers. Cardiomyocyte renewal throughout life is thought to occur mainly through cardiomyocyte division and stem cell proliferation and differentiation into cardiomyocytes. However, upon injury the heart is not able to regenerate and stem cells therapies, which seemed promising, also fail to rescue the failing heart. Hostile microenvironment in the heart might be at the origin of the lack of cardiomyocyte renewal after injury. From Segers V and Lee R, 2008 (66).

Left Ventricular Assist Devices (LVADs)

Ventricular assist devices (VAD) that were developed to support heart function and reduce the pressure overload effects on the heart (FIGURE 4), provide a unique opportunity to understand cardiac endogenous regeneration. Implantation of these devices showed great functional recovery in heart function, including reversal of chamber enlargement and normalization of cardiac structure with reduced stress markers (67–69). A more recent study has evaluated the effect of unloading the heart on the extent of fibrosis and levels of TGF-β. It was demonstrated in this study that unloading the heart significantly reduces the transcription of TGF-β and collagen gene expression as well as a modest reduction in tissue fibrosis (70). Morphologically correlating with the recovery observed in some patients after unloading, prolonged hemodynamic support of the failing heart by LVAD was interestingly associated with reduction in myocyte diameter, size and DNA content (71). Similarly, Wohlschlaeger et al (72) have shown in a bigger patient group that LVAD treatment promotes decrease of cardiomyocyte DNA content and the number of polyploid cardiomyocytes together with an increase in diploid cardiomyocytes (72). This data suggested that upon unloading, the blockade of the cell cycle induced by cardiomyocyte hypertrophy in the failing heart is released allowing karyokinesis and the subsequent cardiomyocyte division (72). Importantly, complete myocyte division demonstrated upon the use of LVADs suggest that myocyte cell cycle is a dynamic process and nuclear polyploidization and cell cycle arrest in the heart are reversible phenomena. Overall, unloading the failing heart has shown success on reversing cardiac remodeling further demonstrating the heart's endogenous capacity for regeneration.

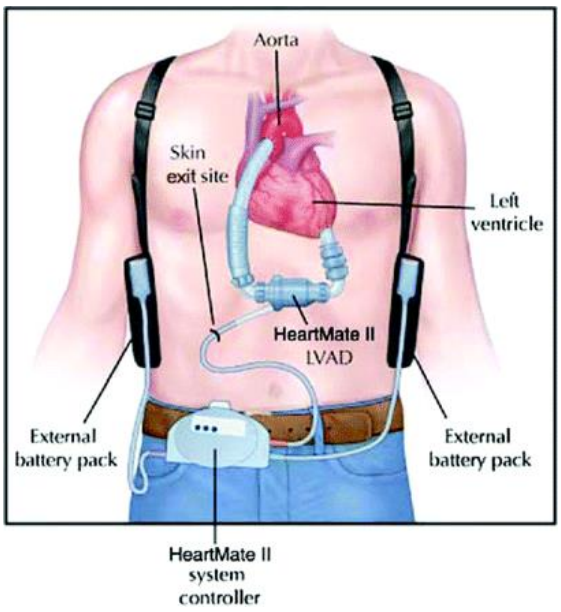

FIGURE 4 | Representation of a commonly used continuous-flow left ventricular assist device. Using the power externally provided by the batteries, the device bypasses the normal circulation of blood from the left atria to the ventricle, reducing pressure overload on the heart. From Givertz M, 2011 (73)

Myocyte Cell Cycle

Initially, during prenatal growth of the heart, hyperplasia of cardiomyocytes (increase in cardiomyocyte numbers through cell division) constitute the main factor contributing for the increase in heart size (74). During fetal life, proliferation of cardiomyocytes occurs rapidly, however this ability to proliferate is lost soon after birth (37). During late prenatal or early postnatal life there is a transition from hyperplasic growth to hypertrophic growth (75). Cardiomyocytes undergo a final round of incomplete cell division which leads to binucleation due to karyokinesis in absence of cytokinesis, culminating in terminal differentiation, in a process called endoreduplication (76). Although the physiological importance of binucleation is still unclear, it has been suggested that it could be an advantageous response to double the capacity of RNA generation in metabolically active cells (37). Concomitantly, cardiomyocytes begin to expand their contractile apparatus, enhancing their excitation contraction efficiency. Moreover, remodeling of extracellular matrix takes place as an effort to adapt to new demands of the heart. This is further reflected in the enlargement of heart chambers and wall and septal thickness (15).

When the switch for hypertrophic growth is completed, which in Humans generally happens before birth, hypertrophy of individual cardiomyocytes becomes the most prominent form of postnatal heart growth (74).

Interestingly, as the heart was envisaged a post-mitotic organ over centuries, there are now evidences showing that there is replacement of cardiomyocytes in the adult heart under normal or increased physiological workload conditions, such as exercise (28). It is now considered that under these situations cardiomyocyte renewal may occur mainly through proliferation of stem cells or proliferation of pre-existent cardiomyocytes, however, the mechanisms that regulate cardiomyocyte renewal are poorly understood.

Compared to what happens in other cell types, cardiomyocyte cell cycle can be divided in G_1, S and G_2 (collectively termed as interphase) and M phase (mitosis). Phase progression is tightly regulated through the transduction of mitogenic signals such as those from IGF-1 or fibroblast growth factor 2 (FGF-2) to cyclins and cyclin-dependent kinases (37). Cyclin-dependent kinases (CDKs) are serine-threonine kinases which upon complexing with the corresponding cyclin, become enzymatically active (37). Cell cycle progression is controlled through a series of checkpoints in which accurate regulation of Cyclins and CDKs is required to ensure specific events at very specific phases (FIGURE 5). This molecular agents act on cell cycle checkpoints that ensure the cell is ready to progress in the cell cycle. The

first checkpoint, termed restriction point, regulates the commitment to enter the cell cycle at late G_1 phase through the assembly of Cdk4 and Cdk6 into holoenzymes preferentially with cyclin D1, D2 or D3 (77). Once assembled into complexes, they drive the release of E2F transcription factors through the phosphorylation of retinoblastoma (Rb) family members (Rb, p107 and p130), enabling them to activate transcription and induce the expression of genes necessary for DNA synthesis and further cell cycle regulators (78). The next checkpoint happens before the start of new DNA synthesis in S-phase, regulating G_1-S phase transition. At this point cyclin E is the most expressed and together with Cdk2 are responsible for accelerating phosphorylation of the Rb proteins. During S-phase, cyclin A is expressed and binds to Cdk2 driving DNA replication. Later on, in late G2 and early M-phase, cyclin A complexes with Cdk1 to direct the entry into mitosis. Thereafter, mitosis is regulated through cyclin B/ Cdk1 complexing. Cyclin/ Cdk activity is further negatively regulated by Cdk inhibitors (Cdki) throughout the whole cycle (37).

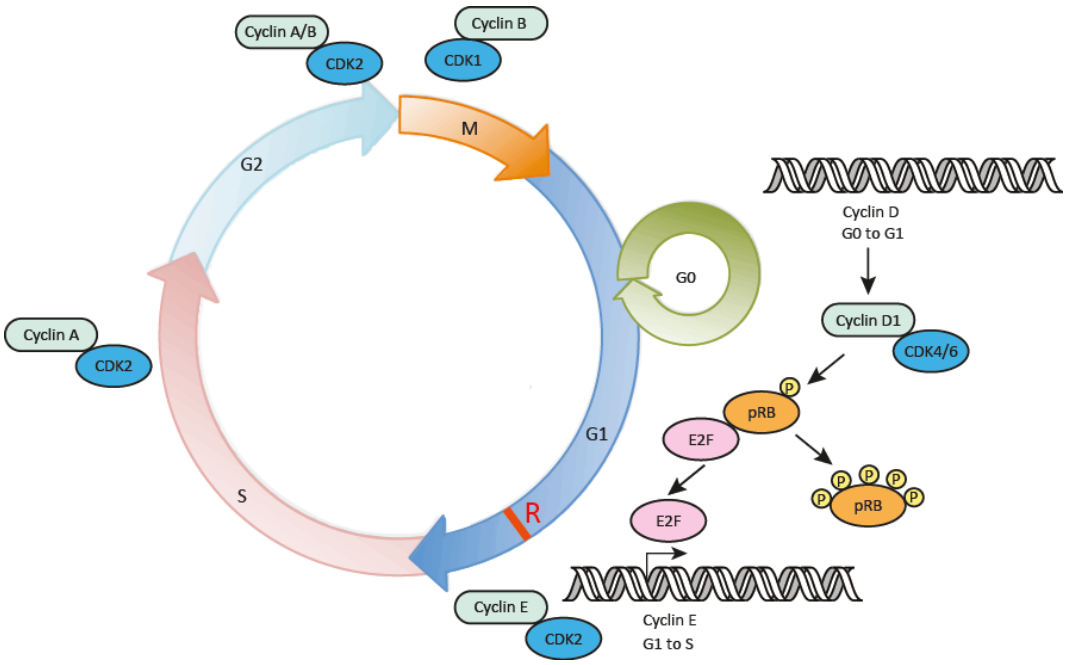

FIGURE 5 | Schematic overview of the cell cycle checkpoints and most well described key regulators. Cyclin and Cyclin-dependent kinases (cdks) interaction through complex formation is tightly regulated throughout the cell cycle to ensure a successful cell division. The specific complexes required at each checkpoint are depicted together with E2F and retinoblastoma (RB) regulation. Adapted from Chiu, J and Dawes, I, 2012 (79)

Research done by multiple research groups pointing out the differences in expression and function of cell cycle regulators during cardiac development provided a new light into how cardiomyocyte cell cycle is regulated.

Expression of cyclins involved in cell cycle (D1, D2, D3 A, B1 and E) and their corresponding kinases was found to be increased in the embryonic heart compared to the adult heart (80, 81). Not surprisingly, upregulation of CdkIs was demonstrated to inversely correlate with the downregulation of cyclins/Cdks during development (77). Cyclin Ds are believed to be expressed throughout the cycle as long as the mitogenic signal is still present. Although mice lacking one of the three isoforms independently of each other are viable with only narrow and tissue-specific phenotype (82), mice lacking all three cyclin D subtypes died during gestation due, in part, to heart abnormalities (83). Conversely, mice overexpressing cyclin D1, D2 or D3 in the adult myocardium showed increased baseline rates of cardiomyocyte DNA synthesis (84). Accordingly, Cdk2 and Cdk4 double knockout mice die during embryogenesis due to hearts defects (85). Overall, it seems that cyclins and Cdks are very important to keep cell division and their reduced expression in adulthood might account for the postnatal withdrawal of cardiomyocytes from the cell cycle.

Along with the changes in cyclin/Cdk expression during development, some different temporal expression patterns are seen for Rb family members, also called pocket proteins. Rb which is the primary target of G1 Cdks is present in very low amounts or undetectable in fetal mouse myocardium at age E12,5 increasing its expression during development, eventually becoming the most expressed pocket protein in the adult myocardium. p107 and p130 are inversely expressed in the myocardium compared with Rb, having both their highest expression during embryonic development decreasing its expression thereafter (86). Rb knockout animals die during gestation as a result of generalized cell death and abnormal cell cycling in different tissues (87). Embryonic stem cells of these animals demonstrated a retarded expression of cardiac-specific transcription factors and, hence, cardiac differentiation. Furthermore, Rb and p130 were shown to have overlapping functions to restrain cell cycle activators and keep quiescence in the adult heart, since mice lacking both proteins displayed a threefold increase in heart weight-to-body weight ratio together with increased numbers of 5-Bromo-2-Deoxyuridine (BrdU) labeled cardiomyocytes and phosphohistone H3 (PH3) positive cardiomyocyte nuclei (88). Taken together, it suggest that Rb proteins might play a role in regulating cell cycle exit and cardiomyocyte differentiation.

Another form of regulation of the cell cycle comes from Myc, which represents the family of sequence-specific DNA-binding proteins, including c-Myc, N-Myc and L-Myc (37). It has been suggested that in the heart, Myc is vital both for cell division and hypertrophy. In fact, embryonic ventricular myocytes express Myc and the expression decreases during development (89). Accordingly, when lacking

it, in c-Myc knockout embryos, cardiac defects are seen that ultimately lead to death of the embryo before term (90). On the other hand, when the expression of c-Myc is induced embryonically and kept overtime in cardiomyocytes, both atrial and ventricular enlargement of these hearts is seen that was further related to myocyte hyperplasia (89). However, it has also been reported that overexpression of proto-ongenes such as Myc may aso result in cell cycle arrest (91). Nonetheless, Myc was overall shown to play an important role in mediating hyperplastic cardiac growth.

A possible endogenous antagonist of Myc is hypoxia inducible factor-1α (HIF-1α). It is a transcription factor that activates or represses the expression of genes that contain hypoxic responsive elements. Although numerous studies have shown that HIF-1α is necessary for hypoxia induced growth arrest and activation of p21 (CdkI that that inhibits the complexes of CDK2 and CDK1), recently a novel function in regulating development cell cycle arrest has been attributed to HIF-1α (92). It has been shown that HIF-1α is able to antagonize Myc action through its displacement from the p21 promoter, inducing cell cycle arrest even in the absence of a hypoxic signal (92). For instance, complete deletion of HIF-1α led to lethality by E11 in HIF-1α -/- embryos as a result of several defects in cardiovascular development including disorganized cardiac morphogenesis with myocardial hyperplasia (93). Furthermore, increased protein levels of HIF-1α have been reported in the heart in different models of cardiac pathologic hypertrophy (94). Although a comprehensive analysis on the role of HIF-1α is still lacking, evidences point for an important role of this transcription factor both in hypertrophy and myocyte proliferation.

Although manipulation of several regulators of the cell cycle described above proved beneficial effects on the cell cycle, a comprehensive analysis should be performed on the most puzzling phase of mitosis in a cardiomyocyte – cytokinesis. This is the final step of cell division that culminates with separation of the cytoplasm between daughter cells to complete mitosis (95), without which myocytes undergo endoreduplication, increasing their ploidy status (37). A study aimed to analyze the differences in sarcomeric structure and contractile ring formation between 2 and 4 days old rats, showed similar pattern of actin organization and formation of ring-like structure in early telophase (96). Therefore, it was suggested that molecules involved in the later stages of cytokinesis might account for the inability of cardiomyocytes to undergo cytokinesis. Furthermore, size differences in cardiomyocytes and thus different complexity of sarcomeric organization may play a role in blocking cytokinesis, since to undergo cytokinesis, cytoskeleton should be disassembled. Accordingly, small mononucleated cardiomyocytes have been

reported in some studies to be the most prominent population of proliferating cardiomyocytes (34, 97).

Nonetheless, the ability of cardiomyocytes to renew throughout life after injury in LVAD patients brings some opportunities for development of approaches to enhance endogenous cardiac regeneration.

CITED4

Nuclear accessibility of some transcription factors and transcriptional co-activators may certainly play an important role on the transcription of pro-proliferative genes to induce cardiomyocyte renewal. Recently, a new member of the CITED family, CREB-binding protein (CBP)/p300-interacting transactivator with ED-rich carboxy-terminal domain 4 (CITED4) that is encoded by a single exon, was described (98). Upon recruitment to a promoter, CITED4 was shown to bind CBP/p300 with high affinity, inducing transcription co-activation. For instance, CITED4 demonstrated ability to co-activate transcription factor AP-2 (TFAP2) (98).

Importantly, CITED4 was found to be significantly increased in exercise models correlated with cardiomyocyte proliferation seen by the increase in ki67 positive cardiomyocytes and increased incorporation of BrdU by cardiomyocytes (32). Moreover, this study has shown that CCAAT-enhancer binding protein-β (C/EBPβ) negatively regulates CITED4 in the heart (32). CITED4 role in cardiomyocyte division was corroborated in a more recent phenotypic screen on rat neonatal cardiomyocytes, where adenoviral overexpression of CITED4 led to increase in ki67 proliferation marker and increased myocyte number (99).

Previous work in this group already showed that transverse aortic constriction (TAC) surgery on mice leads to increased levels of TGF-β and tissue fibrosis along with impaired cardiomyocyte renewal that is associated with increased levels of inhibition of CITED4. Upon unloading, CITED4 levels were restored along with the renewal potential (el Azzouzi H, unpublished).

Main goal and Hypotheses

Considering the importance of tackling the loss of cardiomyocytes and restoring cardiomyocyte renewal after pathological stimuli on the heart, in this project we aim to gain insight on the mechanisms that drive endogenous cardiac regeneration. For this, we perform transverse aortic constriction (TAC) in a mouse group and compare it to their sham operated littermates and to their littermates to whom the ligation was removed after development of the pathological phenotype.

We hypothesize that upon aortic constriction, mice develop a phenotype characteristic of pathological hypertrophy. Moreover, relieving the pressure overload from the heart through the removal of the ligation will lead to restored heart function. Therefore, we believe that by unloading the heart after a sustained pathological stimulation we can further understand what the most striking changes in these hearts are and how regeneration is directed after stress. To elucidate whether cardiomyocyte renewal after pathological stimuli in the heart is regulated by CITED4, we use a cardiac specific deletion of CITED4 together with the unloading model. We further postulate that deletion of CITED4 in the heart will hamper cardiac recovery after unloading possibly through a deranged regeneration potential.

II. Materials and Methods

II. Materials and Methods

Mouse model

CITED4 $^{f/f}$ mice (on a B6CBAF1/J background) were purchased from The European Mouse Mutant Archive (EMMA). Mice harboring a tamoxifen-regulated form of Cre recombinase (MerCreMer) under control of the murine *myh6* promoter (αMHC-MerCreMer; MCM mice)(100) in a B6129F1 background, were used to generate αMHC-MCM-CITED4$^{f/f}$ mice. Adult α-MHC-MCM-CITED4$^{f/f}$ and CITED4$^{f/f}$ mice (10-12 weeks of age) were used for functional and histological analyses. All protocols were performed according to institutional guidelines and approved by local Animal Care and Use Committees. Investigators were blinded to treatment for physiological and biochemical measurements.

Tamoxifen Injection

To induce CITED4 deletion, α-MHC-MCM-CITED4$^{f/f}$ mice were treated with either vehicle (10/90 v/v ethanol/peanut oil, Sigma P2144) or tamoxifen (45 mg/kg per day) by daily intraperitoneal injections for consecutive 5 days prior to unloading. To control for possible tamoxifen effects, CITED4$^{f/f}$ mice were given similar tamoxifen injections.

Transverse Aortic Constriction (TAC) and Unloading procedures

Mice were anaesthetized (ip injection; fentanyl 0.05 mg/kg; dormicum 5 mg/kg; dormitor 0.5 mg/kg) after which transverse aortic constriction (TAC) or sham surgery was performed in 2-3 month-old α-MHC-MCM-CITED4$^{f/f}$ and CITED4$^{f/f}$ mice by subjecting the aorta to a defined 27 gauge constriction between the first and second truncus of the aortic arch as described previously (101, 102). Sham operations were similar except for the constriction of the ligation. Unloading was performed after 7 weeks, using the same surgical protocol after which the ligation was carefully removed.

Echocardiography

For echocardiography, mice were shaved and lightly anaesthetized with isoflurane (mean 1.5% in oxygen) and allowed to breathe spontaneously via a nasal cone. Non-invasive, echocardiographic parameters were measured using a

RMV707B (15-45 MHz) scan-head interfaced with a Vevo-770 high frequency ultrasound system (VisualSonics Inc., Toronto, Canada). Long-axis EKG-triggered cine loops of the left ventricular (LV) contraction cycle were obtained in B-mode to assess end-diastolic/systolic volume. Short-axis recordings of the LV contraction cycle were taken in M-mode to assess wall thickness of the anterior/posterior wall at the mid-papillary level. From B-mode recordings, LV length from basis to apex, LV systolic volume (LVVs) was determined. From M-mode recordings, (FS) was calculated with the following formula: (LVIDd-LVIDs)/LVIDd*100). Ejection fraction (EF) was calculated as ((SV/Vd)*100) with Vs, systolic volume (3,1416*(LVIDs^3)/6)).

Sacrifice and Isolations

Mice were sacrificed by cervical dislocation and the hearts were flushed with PBS. The hearts were divided in two parts: one was snap frozen in liquid nitrogen for further RNA and protein analysis; the other one was fixed in 4% (w/v) paraformaldehyde (PFA) for later use in staining protocols.

Histology

Harvested hearts were perfusion-fixed in 4% (w/v) PFA overnight prior to paraffin-embedding. Paraffin-embedded tissue was cut at 5μm using Microm HM 335 E microtome and the cut pieces were floated in warm distilled water to expand the paraffin cut to its original size. Paraffin-embedded tissue sections were then attached to positively charged microscope slides following by their overnight drying on a warming plate set at 37^{O}C.

Prior to all the staining protocols, tissue slides were deparaffinized through a xylene/alcohol gradient.

Hematoxylin and Eosin staining (H&E)

To evaluate gross morphology of the heart, tissue sections were staining with hematoxylin and eosin. Following deparaffinization, slides were incubated in hematoxylin solution (Klinipath) for 10 min and then washed for 5 min in running tap water. Slides were then incubated for 30 sec in eosin solution [1% (w/v) Eosin yellowish (Gurr Certistain); 70% EtOH (Klinipath); 0,05% (v/v) Acetic Acid (Sigma-Aldrich)]. Finally, slides were washed with distilled water and allowed to dehydrate

through an alcohol/xylene (Klinipath) gradient. Sections were mounted with Entellan (Klinipath).

Picrosirius Red staining

Picrosirius Red staining was used to assess the extent of fibrosis in the hearts. Once deparaffinized, slides were colored in picrosirius red solution [0,1% (w/v) Sirius Red F3B (Gurr); saturated picrine acid solution, pH=2 (Boom)] and washed twice with 0,2N HCl (Sigma-Aldrich) for 5 min followed by 5 min wash with distilled water. From this point on, staining procedure was carried as described for H&E staining.

Immunofluorescent Stainings

Immnofluorescent stainings varied for each antibody used. Details of the antibodies used, dilutions and antigen retrieval methods are described in TABLE 1. Briefly, tissues slides were deparaffinized, followed by antigen retrieval through boiling the slides in the buffer described in the TABLE 1 on a gas burner for 20 minutes. Primary antibody was incubated overnight at 4ºC with the exception of lectin from *Triticum vulgans* (WGA) which was incubated at room temperature for 30 minutes. Goat anti-Mouse Alexa Fluor®488 (1:800, Life Technologies, #A-11001) and goat anti-Rabbit Alexa Fluor®555 (1:2000, Life Technologies, #A-21428) were used as secondary antibodies and were incubated for one hour at room temperature. All sections were counterstained with Hoechst 33342 (1:10000, Life Technologies, #H1399) and mounted with Fluoromount G (Southern Biotech, #0100-01). Negative control sections were included in which the primary antibody was omitted.

TABLE 1 | List of the antibodies and compounds used for immunofluorescent stainings. The antigen retrieval method, blocking buffer and dilution used are also described in detail.

Antigen Retrieval	***Blocking***	***Antibody/ Compound***	***Dilution***
Sodium Citrate (Sigma), pH=6	1%PBSA	Rabbit Monoclonal ab anti-Ki67 (clone SP6) Thermo Scientific #RM_9106_S	1:100 in 0,5%PBSA
Citric Acid (Riedel-de Haën), pH=6	1%TBSA	Rabbit Policlonal ab anti-Phospho-Histone H3 (Ser10) Millipore #06-570	1:200 in 1%TBSA
*	*	Mouse Monoclonal ab anti-Tropomyosin Sigma #T2780	1:200*
Sodium Citrate (Sigma), pH=6	-	Lectin from *Triticum vulgaris* (wheat), FITC conjugate Sigma #L4895	50 µg/ml in 1%PBSA

* - Choice of buffer used depended on the co-staining.

Microscopy and Image Quantification

Pictures of the stained tissues were made using Olympus DP71 camera on an Olympus BX53 microscope.

H&E imaging of the four chamber view of the hearts was done at 10x magnification while regional images were taken at 20x magnification.

Picrosirius Red staining was imaged using polarized light and regional images were made at 20x magnification. Quantification of the fibrotic area was done using ImageJ.

For Ki67 and PH3 staining, at least 20 random pictures were taken at 20x magnification per section or animal and positive cardiomyocyte nuclei were counted in a total of 10000 cardiomyocytes. Nuclei were counted as positive when surrounded by green indicating cardiomyocyte nature.

For WGA staining, 5 to 8 images were taken at 20x magnification per heart or section and cardiomyocyte surface area was measured using an in house made macro on ImageJ. At least a total of 100 cells were measured for each picture taken.

RNA Isolation and RT-qPCR

RNA was isolated using Trizol (Invitrogen) and reverse transcribed using iScript advanced cDNA Synthesis kit for RT-qPCR (BioRad). One microgram of total RNA was used as template for the reverse transcriptase. For quantitative real-time PCR, a Bio-Rad iCycler (Bio-Rad) and SYBR Green were used in combination with specific primer sets TABLE 2 designed to detect transcripts. Quantification was performed using the comparative Cq method with P0 as a housekeeping gene.

TABLE 2 | List of primer sets used and respective melting temperature (T_m).

Gene	***Primers***	***T_m***
cited4	F – CTGATGCTCGCCGAGGGCTAC R – CAGCGGAGCCCCCCGCGGCC	60
acta1	F – CCGGGAGAAGATGACTCAAA R – GTAGTACGGCCGGAAGCATA	60
myh7	F – CGGACCTTGGAAGACCAGAT R – GACAGCTCCCCATTCTCTGT	60
nppb	F – TGGGAGGTCACTCCTATCCT R – GGCCATTTCCTCCGACTTT	60
rcan	F – CCACACAAGCAATCAGGGAGC R – GCTTGACTGAGAGAGCGAGTC	60
P0	F – GGACCCGAGAAGACCTCCTT R – GCACATCACTCAGAATTTCAATGG	60

cited4, Cbp/p300-interacting transactivator, with Glu/Asp-rich carboxy-terminal domain, 4; acta1, α-skeletal actin; *myh7*, β-myosin heavy chain; *nppb*, brain natriuretic peptide; *rcan*, regulator of calcineurin; P0, large subunit ribosomal protein P0. F and R, represent the forward and reverse primer sequences (5' – 3') respectively.

Statistical Analysis

All values were presented as mean ± SEM unless otherwise indicated. All statistical analysis of the results was performed and visualized using GraphPad Prism 6.01. For multiple group comparison, 2way ANOVA test followed by Tukey or Holm-Sidak post hoc test correction for multiple comparisons were performed. Unpaired, two-tailed Student's t test was used to compare two experimental groups. Values of $p<0,05$ were considered significant.

III. Results

III. Results

CITED4 knockout strategy in the heart

Constriction of the transverse aorta is a commonly used surgical procedure that mimics several pathological conditions such as chronic hypertension and aortic stenosis seen in Humans (103). Similarly transverse aortic constriction (TAC) induces chronic pressure overload that leads to left ventricular dysfunction over 4 to 6 weeks in the murine heart (104–106).

Along with decreased function, pressure overload was previously shown to induce cardiac remodeling including fibrosis (107) and cardiomyocyte loss leading thinning of the ventricular walls causing dilatation and eventually heart failure (108). In a recent work by Boström et al (32), the transcriptional co-activator CITED4 was shown to be up-regulated in mice hearts after endurance exercise protocol, correlated with upregulation of cell cycle markers, suggesting a role for maintenance of myocyte division.

Opposite to what was found on a physiological hypertrophy model, previous results in this project show that CITED4 levels are reduced both in human heart failure and in TAC mouse model (el Azzouzi H, unpublished).

To understand what the consequences are of deleting this transcriptional co-activator, we generated cardiomyocyte specific CITED4 deletion through cre-loxP system. In this system, the mice have an α-MHC driven MerCreMer (MCM) expression that is fused to a mutated ligand-binding domain (LBD) of the estrogen receptor (ER). In this system injected tamoxifen binds Cre recombinase and promotes its translocation to the nucleus where it induces recombination and the subsequent removal of the CITED4 loxP flanked region. Since α-MHC is specifically and constitutively expressed in cardiomyocytes, this system ensures an inducible and specific cardiomyocyte knockdown of CITED4 (FIGURE 6).

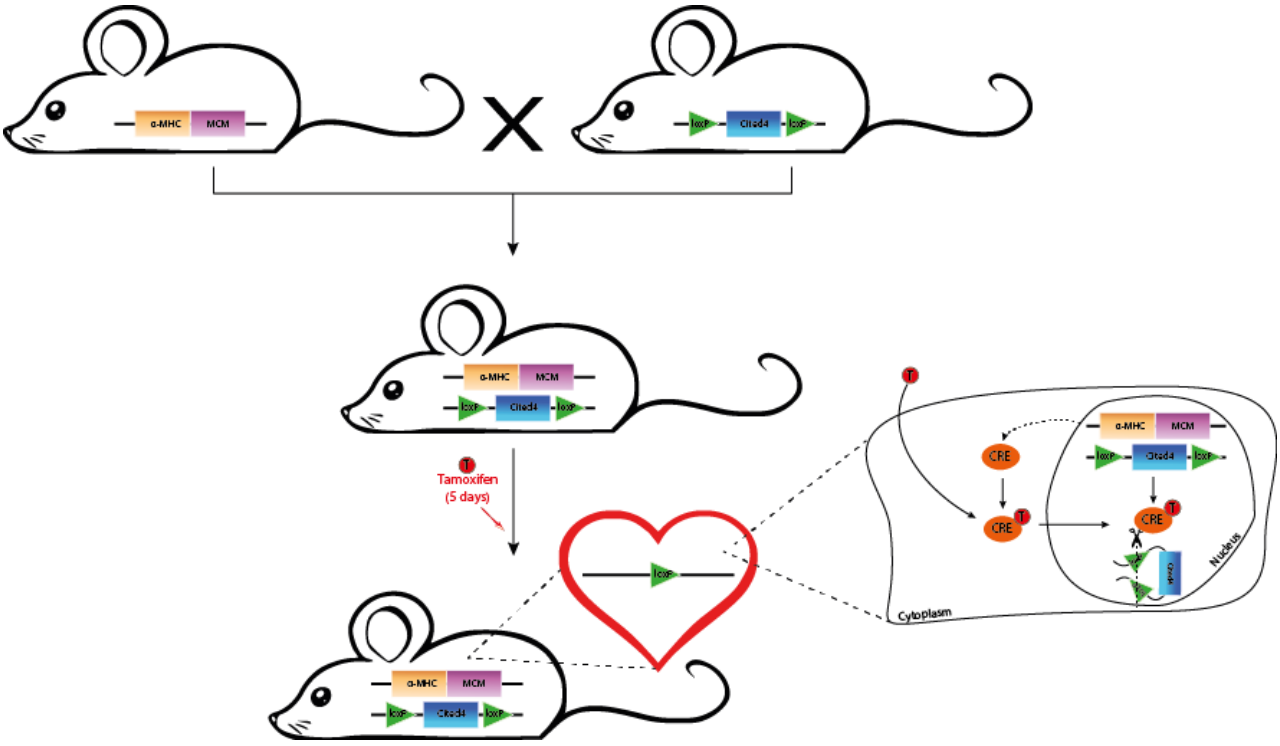

FIGURE 6 | CITED4 knockout strategy in the heart. Schematic representation of the generation of the cardiac specific CITED4 deletion mouse model used. Mice expressing MerCreMer (MCM) driven by α-MHC promoter (α-MHC-MCM) were breed with mice containing CITED4 flanked by 2 loxP sites (CITED4$^{f/f}$), giving rise to α-MHC- MCM-CITED4$^{f/f}$ mice. Injected tamoxifen binds Cre recombinase specifically expressed in cardiomyocytes, promoting its translocation to the nucleus, allowing excision of the loxP flanked CITED4. CITED4$^{f/f}$ mice were used as controls for possible tamoxifen negative effects.

Unloading requires CITED4 to fully restore integrity in the heart

To understand the influence of CITED4 in the heart upon pathological stimuli, α-MHC- MCM-CITED4$^{f/f}$ mice underwent TAC or sham surgery and were left for 6 weeks to develop pathological cardiac remodeling (FIGURE 7 – A). At 6 weeks, a randomly selected group of animals were injected with tamoxifen or vehicle during 5 consecutive days just prior to unloading or sham surgery. This setup allows to specifically assess the role of CITED4 in the unloading induced cardiac regeneration (FIGURE 7 – A). Using this setup, tamoxifen injection resulted in significant knockdown of cited4 transcripts as estimated by real time RT-qPCR (FIGURE 7 – A).

Analysis of the hearts *pos mortem* further showed that TAC induced an increase in size and weight as depicted by gross morphology and heart weight/body weight ratios of both vehicle and Tamoxifen treated α-MHC-MCM-CITED4$^{f/f}$ mice (FIGURE 7 – C,D).

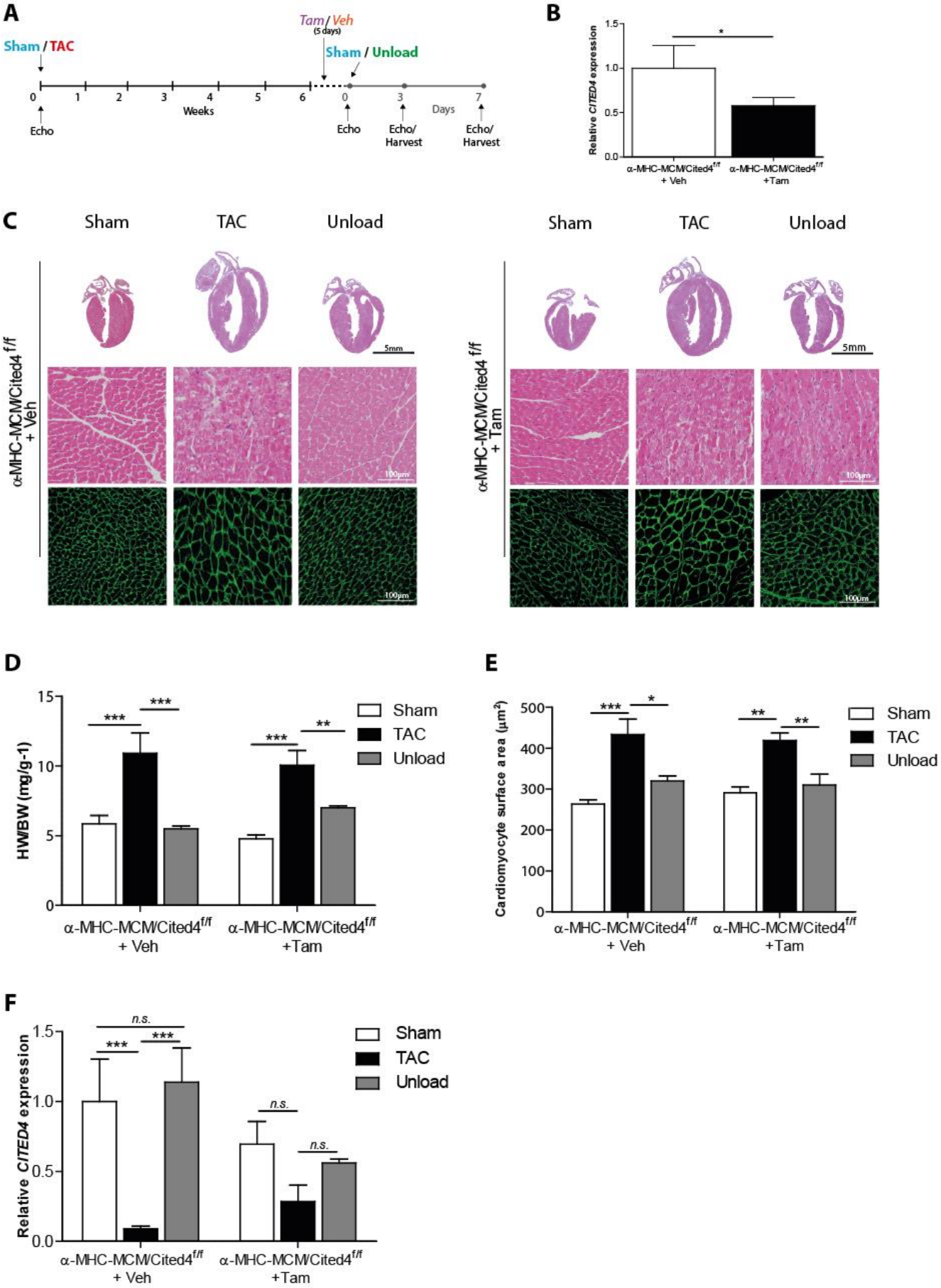
A
Sham / TAC
Tam / Veh
(5 days)
Sham / Unload
0 1 2 3 4 5 6 0 3 7
Weeks
Days
Echo
Echo
Echo/ Harvest
Echo/ Harvest
B
Relative CITED4 expression
1.5
1.0
0.5
0.0
*
α-MHC-MCM/Cited4f/f + Veh
α-MHC-MCM/Cited4f/f +Tam
C
Sham
TAC
Unload
α-MHC-MCM/Cited4 f/f + Veh
α-MHC-MCM/Cited4 f/f + Tam
5mm
100μm
D
HW/BW (mg/g-1)
15
10
5
0
***
***
***
**
Sham
TAC
Unload
α-MHC-MCM/Cited4f/f + Veh
α-MHC-MCM/Cited4f/f +Tam
E
Cardiomyocyte surface area (μm2)
500
400
300
200
100
0
***
*
**
**
Sham
TAC
Unload
α-MHC-MCM/Cited4f/f + Veh
α-MHC-MCM/Cited4f/f +Tam
F
Relative CITED4 expression
1.5
1.0
0.5
0.0
n.s.
***
***
n.s.
n.s.
Sham
TAC
Unload
α-MHC-MCM/Cited4f/f + Veh
α-MHC-MCM/Cited4f/f +Tam

FIGURE 7 | Unloading requires CITED4 to fully restore integrity in the heart. *A*. Schematic representation of the model used, where 6 weeks after TAC or sham surgery, mice are injected with tamoxifen or vehicle and further selected for sham or unloading surgery. Echocardiographies were performed at baseline, pre-unload, 3 days and 7 days after unload. Hearts were harvested either at 3 days or at 7 days; *B*. Quantitative real time PCR analysis of CITED4 transcripts in vehicle treated and tamoxifen treated α-MHC-MCM-CITED4$^{f/f}$ hearts (n=13/group) indicating significantly reduced CITED4 transcripts in tamoxifen treated α-MHC- MCM-CITED4$^{f/f}$ mice; *C*. Representative histological images of sham, TAC and unloaded mice of indicated genotypes and treatments, 7 days after the unloading time-point. *Top pannels*, representative four chamber view images of the hearts, indicating enlargement of the heart upon TAC that is reverse after unload. *Scale bars*, 5 mm. *Middle pannels*, Hematoxylin and eosin-stained images reveal remarkable myocyte hypertrophy and myofiber disarray in mice subjected to TAC surgery that is reversed upon unloading only in vehicle treated group. *Scale bars*, 100µm. *Lower pannels*, representative images of WGA-labeled tissue sections. *Scale bars*, 100µm; *D*. Heart weight/body weight ratios of sham, TAC and unload mice of indicated genotypes and treatments, 7 days after the unloading time-point, indicating a significant increase in cardiac mass after pressure overload that is further decreased upon unloading (*n* = 6-9/group); *E*. Quantification of individual cardiomyocyte surface area (µm^2), showing hypertrophy of individual cardiomyocytes upon TAC that is reversed after unloading; *F*. Quantitative real time PCR analysis of *CITED4 transcripts* in hearts of sham, TAC and unloaded mice of indicated genotypes and treatments, 7 days after the unloading time-point, indicating that vehicle treated α-MHC-MCM-CITED4$^{f/f}$ mice decrease CITED4 transcripts after TAC and further increase transcripts to sham levels after 7 days of unloading. Tamoxifen treated α-MHC-MCM-CITED4$^{f/f}$ mice show lower levels of CITED4 in all time-points. *Error bars* are represented as Mean ± SEM; *n.s.*, not significant; * p<0,05; ** *p*<0,01; ***p<0,001.

Considering the fact that pressure overload is associated with cardiac remodeling, we further looked into cell integrity. Hematoxylin and eosin (H&E) staining showed that cardiomyocytes lose integrity upon TAC-induced pressure overload when compared to sham hearts (FIGURE 7 – C). Unloading the vehicle treated α-MHC-MCM-CITED4$^{f/f}$ mice fully restored size and reduced signs of histopathology in cardiomyocytes (FIGURE 7 – C, D). Although, tamoxifen treated α-MHC-MCM-CITED4$^{f/f}$ mice showed diminished heart size compared to their TAC cohorts, individual cardiomyocytes displayed signs of disintegration (FIGURE 7 – C, D). WGA staining was performed to visualize cell membranes and allow measurement of the individual cardiomyocyte surface area. Similarly, cardiomyocyte surface area increased upon TAC (FIGURE 7 – C, E), indicating a hypertrophic response which possibly accounts for the increase in size and weight of these hearts (FIGURE 7 – C, D). Unloading the hearts promoted a decrease in cardiomyocyte surface area, indicating regression of hypertrophy in both vehicle and tamoxifen treated α-MHC-MCM-CITED4$^{f/f}$ mice (FIGURE 7 – C, E). Strikingly, although removal of pressure overload caused a reduction in heart size, individual

cardiomyocytes from tamoxifen treated α-MHC-MCM-CITED4$^{f/f}$ mice displayed severe disintegration (FIGURE 7 – C).

Given the fact that cardiomyocyte disintegration is persistent both in TAC surgerized mice and CITED4-deficient unloaded hearts suggests a role for CITED4 in cardiomyocyte physiology following injury. Indeed, *cited4* transcript levels were reduced upon TAC surgery and restored after unloading in vehicle treated α-MHC-MCM-CITED4$^{f/f}$ mice but not in tamoxifen treated α-MHC-MCM-CITED4$^{f/f}$ mice (FIGURE 7 – F).

Cardiomyocyte disarray has been considered to drive tissue loss in failing hearts which is also hallmarked by extensive fibrosis (109). To evaluate whether these hearts have developed fibrosis, we performed picrosirius red staining on cardiac sections of all mice cohorts. Pressure overloaded mice hearts showed extensive interstitial fibrosis which was reversed to sham levels after 7 days of unloading of vehicle treated α-MHC-MCM-CITED4$^{f/f}$ mice (FIGURE 8 – A, B). Strikingly, tamoxifen treated α-MHC-MCM-CITED4$^{f/f}$ mice showed no significant reduction of fibrotic area (FIGURE 8 – A, B). Fibrotic quantification of tamoxifen treated α-MHC-MCM-CITED4$^{f/f}$ mice that were sham operated showed comparable fibrotic events to their vehicle treated cohorts (FIGURE 8 – A, B).

Next to fibrosis and cardiomyocyte disarrangement, reactivation of fetal gene expression characterizes pathological remodeling of the heart. To assess this, transcript levels of *nppb* (brain natriuretic peptide), *myh7* (β-myosin heavy chain), *rcan* (regulator of calcineurin) and *acta1* (α-skeletal actin) were analyzed using qPCR (FIGURE 8 – C-F). In general, all genes were found to be up regulated after pressure overload in both vehicle and tamoxifen treated α-MHC-MCM-CITED4$^{f/f}$ mice (FIGURE 8 – C-F). Unloading resulted in reduced transcript levels of these stress markers in vehicle treated α-MHC-MCM-CITED4$^{f/f}$ mice (FIGURE 8 – C-F) coherent with the reverse remodeling observed in these hearts indicated by lower cardiomyocyte disarray (FIGURE 7 – C) and reduced fibrosis (FIGURE 8 – A, B). On the other side, unloading of tamoxifen treated α-MHC-MCM-CITED4$^{f/f}$ mice showed no reversal of *acta1*, *myh7, nppb* and *rcan* transcript levels (FIGURE 8 – C-F).

Taken together, these data points CITED4 to be crucial for the beneficial effects of unloading the heart including maintenance of cardiomyocyte integrity, reversal of fibrosis and stress markers.

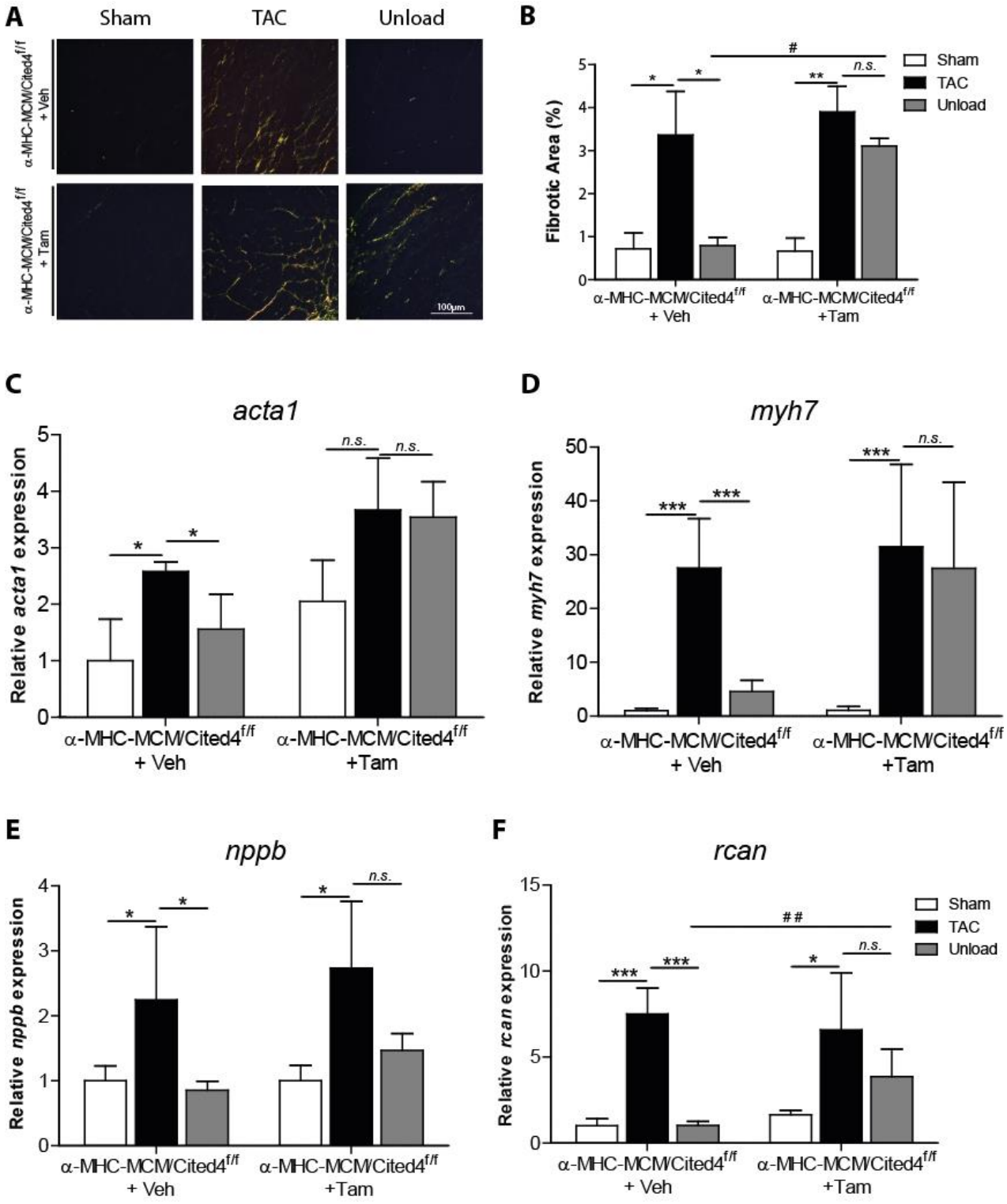

FIGURE 8 | Persistent fibrosis and altered stress marker transcripts in cardiac CITED4-deficient mice upon unloading. *A*. Representative picrosirius red staining histological images of sham, TAC and unloaded mice of indicated genotypes and treatments, 7 days after the unloading time-point, showing great extension of intersticial fibrosis upon TAC and after unload in the tamoxifen treated α-MHC-MCM-CITED4$^{f/f}$ mice. *Scale bars*, 100μm; *B*. Quantification of extension of fibrosis (%) in the hearts, indicating an increase in fibrotic area in TAC that is reversed in vehicle treated animals but not

in tamoxifen treated α-MHC- MCM-CITED4$^{f/f}$ mice (n=4-7/group; n=2 for tamoxifen treated α-MHC-MCM-CITED4$^{f/f}$ sham operated mice); *C–F*. Quantitative real time PCR analysis of (*C*.) *acta1* (α-skeletal actin), (*D*.) *nppb* (brain natriuretic peptide) and (*E*.) *myh7* (β-myosin heavy chain) and (*F*.) *rcan* (regulator of calcineurin) in hearts of sham, TAC and unloaded mice of indicated genotypes and treatments, 7 days after the unloading time-point, indicating increased transcript levels of these stress markers after TAC that is fully reversed in vehicle treated α-MHC-MCM-CITED4$^{f/f}$ mice after unload (n=5-6/group). Tamoxifen treated α-MHC-MCM-CITED4$^{f/f}$ mice showed transcript levels of *acta1*, *nppb*, *myh7* or *rcan* after unloading comparable to TAC operated animals. *Error bars* are represented as Mean ± SEM; *n.s.*, not significant; * p<0,05; **/ ## *p*<0,01; ***p<0,001.

Aortic constriction induces pathological remodeling that requires CITED4 for a full recovery upon unloading

To functionally determine the effect of CITED4 knockdown on pressure overload-induced hemodynamic changes in the heart, we performed M-mode echocardiography at 7 weeks after TAC (prior to unloading) and at 3 and 7 days following unloading (FIGURE 7 – A). Representative images of M-mode recordings of all experimental groups are displayed in FIGURE 9. Pressure overloaded mice hearts showed ventricular wall thinning characterizing end-stage heart failure which was fully reversed to sham levels after 7 days of unloading of vehicle treated α-MHC-MCM-CITED4$^{f/f}$ mice (FIGURE 9 – A). Interestingly, although tamoxifen treated α-MHC-MCM-CITED4$^{f/f}$ mice showed some increase in ventricular wall dimensions, this was not comparable to their vehicle treated counterparts (FIGURE 9 – A).

In line, measurements at 7 weeks showed reduced cardiac contractility of the TAC operated vehicle or Tamoxifen treated α-MHC-MCM-CITED4$^{f/f}$ mice. Both ejection fraction (FIGURE 9 – B) and fractional shortening (FIGURE 9 – C), which represent the percentage of blood that is pumped out of the left ventricle in each contraction and the difference in ventricular diameters in systole and diastole, respectively were reduced after 7 weeks of pressure overload. Unloading the TAC hearts allowed the vehicle treated α-MHC- MCM-CITED4$^{f/f}$ mice to fully recover cardiac function within 3 to 7 days as depicted by left ventricular ejection fraction and fractional shortening (FIGURE 9 – B, C). However, tamoxifen treated α-MHC-MCM-CITED4$^{f/f}$ mice showed impaired functional recovery within the same period of time (FIGURE 9 – B, C). Interestingly, although tamoxifen treated α-MHC-MCM-CITED4$^{f/f}$ mice showed impaired recovery after 3 days of unloading, cardiac contractility increased in the following 4 days, indicating delayed recovery in these hearts (FIGURE 9 – B, C). In line with the observed early recovery, vehicle treated α-MHC-MCM-CITED4$^{f/f}$ mice showed maintenance of recovery of cardiac function

reaching sham levels. In contrast, tamoxifen treated α-MHC-MCM-CITED4$^{f/f}$ mice did not recover to sham levels even after 7 days of unloading (FIGURE 9 – B, C). Sham operated animals maintained their cardiac function throughout the whole procedure irrespective of tamoxifen treatment advocating a prominent role of CITED4 in the healing process. Coherent with the findings on the contraction parameters, α-MHC-MCM-CITED4$^{f/f}$ pressure overloaded hearts showed severe increase in left ventricular internal volume in systole (LViVs) regardless of tamoxifen treatment (FIGURE 9 – D). Unloading vehicle treated α-MHC-MCM-CITED4$^{f/f}$ hearts showed a more prominent decrease in LViVs than their tamoxifen treated counterparts reaching sham levels within 7 days. Together, these data suggests that functional recovery coincides with structural improvement seen in vehicle but not in tamoxifen treated α-MHC-MCM-CITED4$^{f/f}$ mice.

Considering the differences in the recovery of unloaded α-MHC-MCM-CITED4$^{f/f}$ mice with respect to their treatment, CITED4 may be proposed as an early mediator in the healing process that may function together with transcriptions factors to initiate recovery.

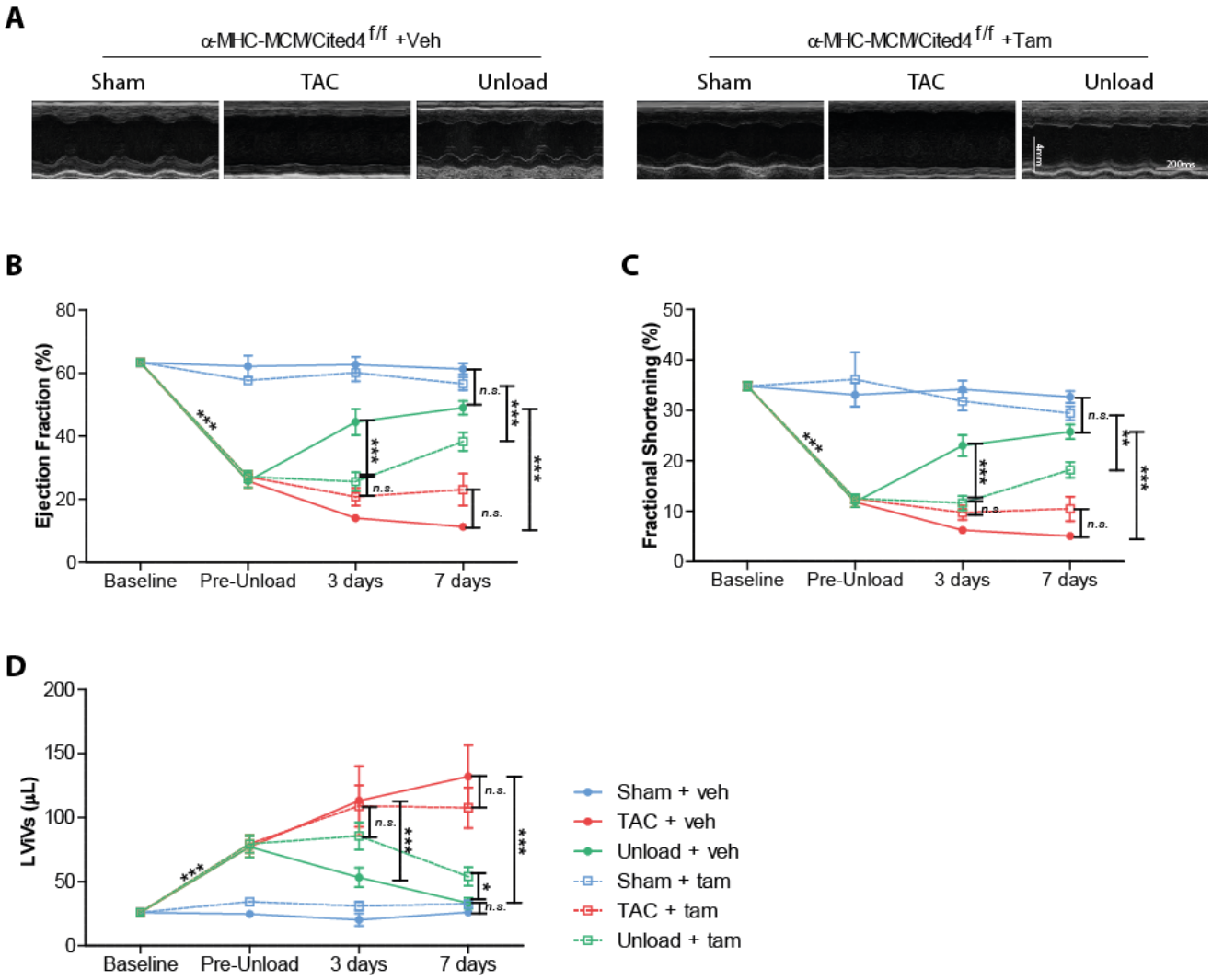

FIGURE 9 | Aortic constriction induces decrease of heart function that requires CITED4 for a full recovery upon unloading. *A*. representative M-mode images of mice with the indicated genotype and treatment 7 days after the unloading time-point, indicating increased LV internal dimensions after pressure overload that are reversed upon unloading for both treatments. *Time scale* and *size* indication are depicted in the M-mode images. *B-D*. Graphical representation of (*B*.) fractional shortening (FS), (*C*.) ejection fraction (EF) and (*D*.) LV internal volume at systole (LViVs), indicating increased functional and geometrical deterioration after TAC that is completely reversed in vehicle treated α-MHC-MCM-CITED4$^{f/f}$ mice within 3 to 7 days of unloading and not fully in tamoxifen treated α-MHC-MCM-CITED4$^{f/f}$ mice (n=5 – 9/ group). *Error bars* are represented as Mean ± SEM; *n.s.*, not significant; * p<0,05; ** *p*<0,01; ***p<0,001.

To control for the possible effect of tamoxifen on the mice, CITED4$^{f/f}$ mice were treated as previously described for the study groups (FIGURE 7 – A). Echocardiographic data from these animals showed no differences compared to the vehicle treated α-MHC-MCM-CITED4$^{f/f}$ mice of all conditions (sham, TAC, unload) (Supplementary FIGURE 11), indicating that tamoxifen treatment on itself did not influence cardiac function before or after unloading. Considering that CITED4$^{f/f}$ tamoxifen injected mice did not develop any cardiac relevant alterations when compared to vehicle treated α-MHC-MCM-CITED4$^{f/f}$ mice, only α-MHC-MCM-CITED4$^{f/f}$ genotype was further investigated.

Unloading related functional outcomes are associated with myocyte division

Previous work in the group showed that unloaded hearts display a significant increase in cycling cardiomyocytes in the myocardium compared to sham operated or pressure overloaded hearts (el Azzouzi, H, unpublished). Unloading the heart through LVAD in Humans was also shown to induce cardiomyocyte proliferation and further division, reducing the number of multinucleated cardiomyocytes and polyploid nuclei within the same cardiomyocyte (71, 72), further proposing cardiomyocyte re-entry in the cycle as a mechanism by which cardiomyocyte renewal is achieved in the unloaded hearts. Although stem cell activation and mobilization are generally pointed as a source for cardiomyocyte renewal, previous work in the group did not find evidences of major stem cell contribution to the healing process in these hearts (el Azzouzi, H, unpublished).

To understand whether the impaired recovery seen in cardiac CITED4-deficient mice is related to attenuated cardiomyocyte renewal, we investigated the proliferative capacity of cardiomyocytes in these hearts by immunofluorescence imaging of Ki67, a marker for active cell cycle. Although unloaded hearts of vehicle

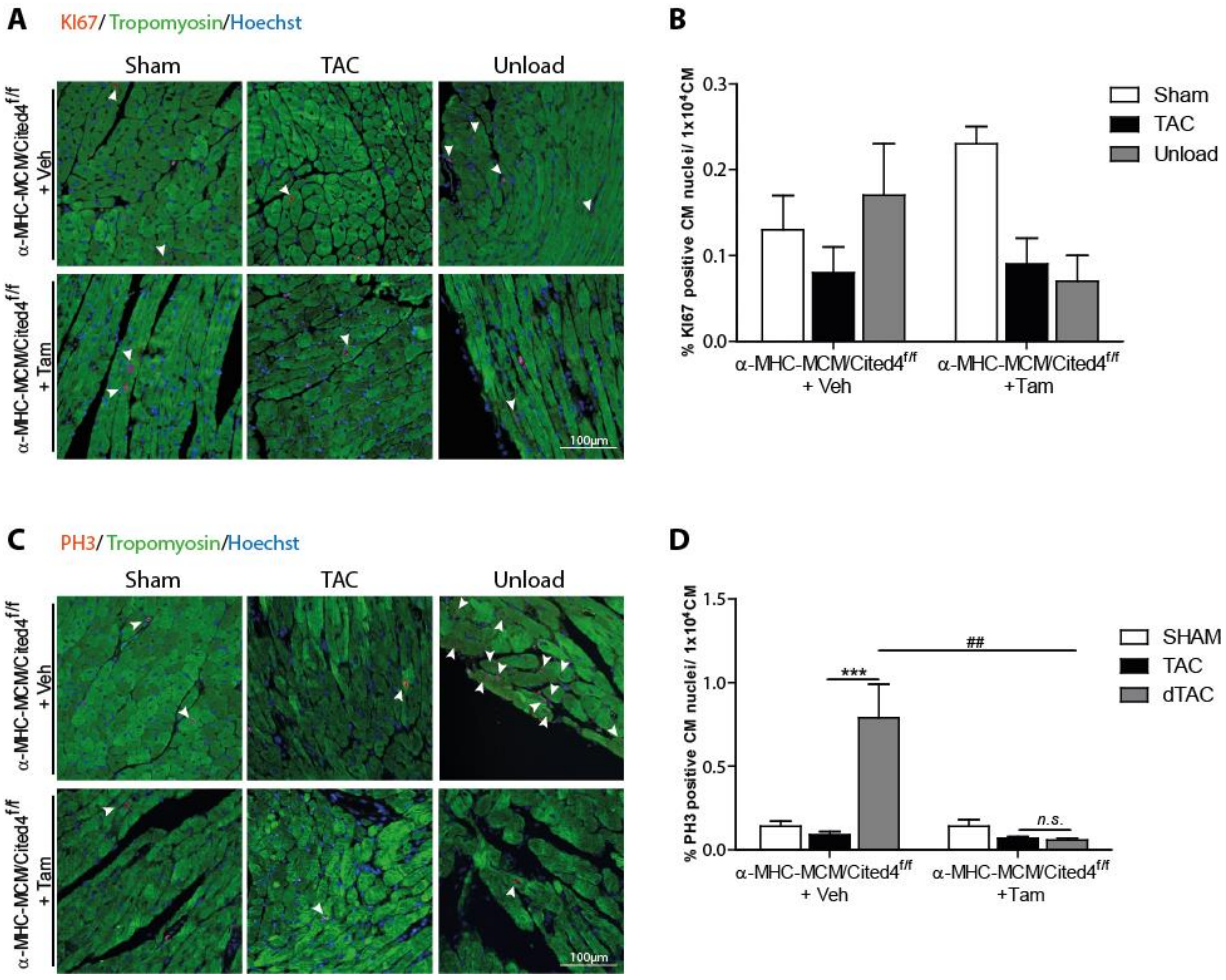

FIGURE 10 | Unloading related functional outcome is associated with myocyte division. *A*. Representative images from immunofluorescent staining for Ki67 of sham, TAC and unloaded mice of indicated genotypes and treatments, 3 days after the unloading time-point. *Scale bars*, 100µm; *B*. Quantification of the number of Ki67 positive cardiomyocyte nuclei per 10000 cardiomyocytes (%)(n=4-7/group); *C*. Representative images from immunofluorescent staining for phospho-histone H3 (PH3) of sham, TAC and unloaded mice of indicated genotypes and treatments, 3 days after the unloading time-point. *Scale bars*, 100µm; D. Quantification of the number of PH3 positive cardiomyocyte nuclei per 10000 cardiomyocytes (%) (n=4-7/group); *Error bars* are represented as Mean ± SEM; *n.s.*, not significant; ## *p*<0,01; ***p<0,001.

treated α-MHC-MCM-CITED4$^{f/f}$ mice showed a prominent increase in numbers of ki67 positive cardiomyocyte nuclei compared to pressure overloaded hearts, this was not significant (**FIGURE 10** – A, B). On the other hand tamoxifen treated α-MHC-MCM-CITED4$^{f/f}$ hearts showed very low numbers of ki67 positive cardiomyocyte nuclei, at a comparable level to their pressure overloaded counterparts (**FIGURE 10** – A, B).

In general, cell cycle activation has been shown by several groups to be required for cardiomyocyte renewal. However, cell cycle is a dynamic process that is thoroughly controlled at several checkpoints and thus activation of the cell cycle

solely is insufficient for completing myocyte division. A more relevant approach to cardiomyocyte division in these hearts was done through immunofluorescent imaging of Phosphoshistone H3 (PH3), a marker for mitosis. Interestingly, vehicle treated α-MHC-MCM-CITED4$^{f/f}$ mice showed a striking significant increase in PH3 positive cardiomyocyte nuclei number compared to sham operated or TAC operated mice (**FIGURE 10** – C, D). However, α-MHC-MCM-CITED4$^{f/f}$ mice treated with tamoxifen showed very low counts of PH3 positive cardiomyocyte nuclei, displaying similar numbers to what is seen for their sham operated and pressure overloaded counterparts (**FIGURE 10** – C, D). Overall, these data suggests CITED4 as a major player in cardiomyocyte cell cycle progression through mitosis.

IV. Discussion

IV. Discussion

Despite intense research on mechanisms underlying cardiac regeneration over the past years, this process remains poorly understood. The discovery of stem cells in the adult heart and the fact that renewal of cardiomyocytes is maintained throughout life contradicted the initial thought that the heart was a post mitotic organ and brought a new avenue for cardiac regeneration research. However, upon injury endogenous stem cells are insufficient to restore cardiac function and the same is often seen in clinical trials upon injection of exogenous stem cells in the heart after injury (57, 58). It is therefore of utmost importance to understand the mechanisms that underlie cardiomyocyte renewal.

On the other hand, by reducing the demand on the heart, LVADs have been shown to improve recovery after injury through cardiomyocyte division and removal of fibrosis. In this light, the possibility of regenerating the heart and the study of the mechanisms that regulate cardiomyocyte renewal herein are becoming increasingly relevant.

Here we describe a unique model to comprehensively understand the mechanisms that drive endogenous cardiac regeneration. α-MHC-MCM-CITED4$^{f/f}$ mice underwent TAC or sham surgery and were left for 6 weeks to develop the pathological phenotype. At 7 weeks, they were injected with tamoxifen or vehicle with single injections for five consecutive days. Following this, a group of mice were selected for further unloading while the others were sham operated. Injection of tamoxifen ensures specific cardiomyocyte deletion of CITED4 immediately before unloading the heart, allowing the precise study of the effect of this transcription co-activator in the recovery process.

Coherent with previous work on the unloading model, vehicle treated α-MHC-MCM-CITED4$^{f/f}$ mice showed an exceptional recovery 3 days after unloading which was comparable to sham levels after 7 days. However, mice lacking CITED4 in the heart showed blunted recovery, with no significant recovery after 3 days and only showing some improvement in function thereafter. Functional measurements reflected the observed dilatation, individual cardiomyocyte disarrangement and persistence of fibrosis seen after unloading cardiac specific CITED4 knockout hearts.

CITED4 was recently investigated in a physiological hypertrophy model where its expression in the hearts was linked to increased number of mitotic cardiomyocytes after an exercise protocol. Our work showed that both Ki67 and PH3 positive cardiomyocyte nuclei were increased after unloading in the vehicle

treated α-MHC-MCM-CITED4$^{f/f}$ mice but not in tamoxifen treated cohorts. Although Ki67 did not show any statistically significant change between groups, which would possibly be solved by increasing the population size per condition, the depicted trend suggests cardiomyocyte re-entry in the cell cycle.

Since Ki67 is expressed from G1 until the end of M phase, quantification of the number of cardiomyocytes expressing this marker does not give any information about the cell cycle phase of the individual cardiomyocyte. In fact, several groups have reported the number of Ki67 positive cardiomyocyte nuclei to be increased in the border zone of a myocardial infarct (36, 110), however, these cycling cardiomyocytes are not enough to restore cardiac function and ultimately cardiac tissue loss is the most prominent phenomenon. Indeed, pathological stimuli on the heart induces hypertrophy of cardiomyocytes which initially promotes cell cycle activation, increasing the DNA content per nuclei or the nuclei per cell. Increasing DNA content per cell might be beneficial in terms of fast mRNA production for future protein translation. However, the increase in cardiomyocyte and nuclei size which is concomitant with a decrease in contractile function exacerbates the stress stimuli on the neighboring cardiomyocytes inducing tissue loss. In this light, actual cardiomyocyte division is crucial for keeping the cardiomyocyte physiology and to functionally restore the damaged myocardium. Accordingly, the findings observed with immunofluorescent imaging of PH3 positive cardiomyocyte nuclei in this study explain the differences in the recovery profile of α-MHC-MCM-CITED4$^{f/f}$ mice respective to the treatment. Since PH3 is only expressed by cells undergoing mitosis, it therefore represents a valid detection method for dividing cardiomyocytes. Functionally, it is intriguing to see that the great functional improvement of vehicle treated α-MHC-MCM-CITED4$^{f/f}$ hearts upon unloading is hampered in the absence of CITED4, which is marked by the inability to complete cardiomyocyte division. To further assess cytokinesis in these models, additional stainings such as Aurora B marker could potentiate the understanding of the proliferative capacity of cardiomyocytes herein.

Another interesting point to evaluate in this model is the polyploidy status and multinucleation of the cardiomyocytes. Work on LVAD use in patients suggest that polyploidy status decrease together with a decrease in the number of multinucleated cardiomyocytes in the myocardium (71, 72), suggesting the relevance of division of pre-existing cardiomyocytes over stem cell proliferation and differentiation into cardiomyocytes. Therefore, it would be valuable to verify whether the same holds true in our unloading model and whether CITED4 has a specific role herein.

Statistically significant changes were not found in the counts for ki67 or PH3 positive cardiomyocyte nuclei between sham operated and TAC operated animals from both groups. This data suggests that cardiomyocyte turnover might be maintained during pressure overload in the heart. However, this prolonged stress stimuli induces a pathological response in cardiomyocytes which shifts the normal turnover balance of cardiomyocytes towards a cell death outcome that is pronounced in TAC but not in sham operated animals regardless of the treatment. Furthermore, CITED4 knockout in the heart at a short time point does not hamper cardiomyocyte division under physiological (sham) or pathological (TAC) conditions. In fact, considering the natural decrease of CITED4 in the heart upon TAC in vehicle treated α-MHC-MCM-CITED4$^{f/f}$, differences in outcome due to CITED4 knockout in the heart were not expected, which was further supported by our data.

There is a long standing belief among the scientific community that left ventricular hypertrophy (LVH) regression brings beneficial effects in the function of the heart. However the actual functional significance of LVH in the recovery from heart failure has never been accurately appreciated (111). In this work we show that unloading reverses hypertrophy regardless of the treatment. Quite surprising was the fact that although tamoxifen treated α-MHC-MCM-CITED4$^{f/f}$ mice significantly decreased their heart weight/ body weight ratio, heart and individual cardiomyocyte size upon unloading, comparable to vehicle treated mice, they did not show a great functional recovery. Considering the observations on our model, we suggest that unloading the pressure overloaded heart is enough to remove the stress environment in the heart allowing the cessation of the pathological pro-hypertrophic stimuli that keeps the cardiomyocytes hypertrophied. Therefore unloading the heart is sufficient to cause regression of hypertrophy regardless of the treatment. Moreover, one might postulate that hypertrophy is required to cope with the increased demand on the heart seen under pathological conditions and its regression is a natural response after relief of this pressure.

Nevertheless, it remains extremely intriguing to understand the mechanisms that underlie this regression and the long term effects on muscle physiology in general.

In accordance with the reduced functional recovery after unloading on tamoxifen treated α-MHC-MCM-CITED4$^{f/f}$ mice, stress marker (*acta1*, *myh7*, *nppb* and *rcan*) expression did not reverse to sham levels in these animals. On the other hand, vehicle treated α-MHC-MCM-CITED4$^{f/f}$ mice demonstrated complete reversal of all the markers 7 days after unloading. Similarly, lowered levels of *myh7* and *nppb* in patients that underwent LVAD support were previously reported (112). This data

suggests that fetal gene reprogramming that is induced upon TAC, is reversed upon unloading dependent of CITED4. In line, it can be postulated that relief of pressure overload in the heart is not sufficient to lower stress marker expression in the heart.

Fibrosis has been described as a characteristic of heart failure in several pathological models, however its exact role in heart failure is still under debate. Another evidence of failure in the rescue of pressure overloaded cardiac CITED4-deficient mice lies in the fact that extensive fibrosis was persistent after unloading significantly differing from the reduced fibrotic area seen in vehicle treated α-MHC-MCM-CITED4$^{f/f}$ mice. The extensive fibrosis areas seen in these animals might account for the lack of functional improvement since scar tissue is not contractile and although it helps keeping the integrity of the heart, it does not support its pumping function.

Considering the different cardiomyocyte division profile seen in these two groups of animals, it can be proposed that in the absence of CITED4 in the heart, the previously existing fibrosis due to pressure overload is not replaced by new functional cardiomyocytes at the same rhythm as it is in their vehicle treated counterparts and thus fibrotic events are predominant. Another possible explanation for persistence of fibrosis after unloading in tamoxifen treated α-MHC-MCM-CITED4$^{f/f}$ mice could be the induction of cardiomyocyte death and replacement with fibrosis. In this setting, additional experiments to measure cell loss in our model could should shed a light on the complex relation between tissue loss and fibrosis on one hand and cardiomyocyte renewal on the other hand.

Cardiac hypertrophy and fibrosis are associated with the induction of myocardial TGF-β synthesis that is consistently highly upregulated in animal models of heart failure (113). Previous data showed that unloading the pressure overloaded heart decreases the levels of TGF-β which was concomitantly linked with reduced fibrosis in these animals (114)(el Azzouzi H, unpublished). It would be relevant to verify whether TGF-β levels differ between the treated groups and whether this reflects the removal of fibrosis in vehicle treated but not tamoxifen treated α-MHC-MCM-CITED4$^{f/f}$ mice or the observed regression of hypertrophy of both unloaded groups.

Previously in the group TGF-β signaling has been shown to indirectly inhibit CITED4 through the activation of miR-24 (el Azzouzi H, unpublished). Accordingly, different group showed that silencing miR-24 in vivo through antagomir therapy in a TAC model prevented the decrease in cardiac function seen in a later stage of TAC (115). Considering this, future experiments should be designed to evaluate the interaction between miR-24 and CITED4 and whether differences in miR-24

expression could underlie the delayed recovery seen in tamoxifen treated α-MHC-MCM-CITED4$^{f/f}$ mice.

miR-222 is another micro-RNA that may be relevant to assess using the model described in this work. It was recently reported that miR-222 increases in mice following exercise protocol and the expression of this miR was linked to an increase in PH3 numbers one week after ischemia injury. Moreover, expression profiling depicted a CITED4 induced increase by miR-222, indicating that miR-222 acts upstream CITED4 (116). Therefore, it would be of great interest to verify whether miR-222 has a role in the recovery process induced by unloading in vehicle treated α-MHC-MCM-CITED4$^{f/f}$ mice probably through the activation of CITED4.

Next to a change in micro-RNA profiling upon unloading, long non-conding RNAs (lncRNA) were found to be markedly altered in response to LVAD support (117). The same authors demonstrated that lncRNA expression signature discriminates failing hearts from hearts that recovered with LVAD support (117). Although not a lot is known concerning the function of specific lncRNAs in the heart, evaluating the expression profile of lncRNAs in our model would bring a new avenue for future research on the mechanisms underlying cardiac regeneration upon relief of pressure overload in the heart.

CITED4 has just recently raised attention and therefore there is not a lot known on its upstream activation or downstream targets. Our model would provide a valuable tool to investigate the key activators of CITED4 re-expression after unloading and the possible downstream targets. IGF-1, which is highly recognized to take a role in physiological hypertrophy, would be a candidate to be further analyzed as a possible upstream activator of CITED4 expression, since it is known to regulate several cell cycle genes that were upregulated upon CITED4 expression, such as cyclin-D1, E2F and myc family members (32, 118, 119). TFAP2 was shown to be co-activated by CITED4 (98) and thus, it might be postulated that it may promote TFAP2 regulated gene transcription. Considering that CITED4 showed a promising role on cardiomyocyte division, the expression of genes regulated by TFAP2 that are known to play a role in cell cycle might be a valuable tool to investigate possible downstream targets of CITED4 and their importance on cardiomyocyte renewal.

Overall, although our setup does not allow to investigate the long term deletion of CITED4 under normal or pathological conditions, it points CITED4 as a major player in the recovery process in pressure overloaded hearts.

V. Conclusions & Future Perspectives

V. Conclusions and Future Perspectives

In this work we describe a unique model consisting of unloading a pressure overloaded heart that enables the study of the mechanisms that drive endogenous cardiac regeneration. Indeed, the exceptional functional outcome observed after unloading the vehicle treated α-MHC-MCM-CITED4$^{f/f}$ TAC surgerized hearts supports the dynamic state of the heart and its endogenous regeneration potential.

CITED4 is a transcription co-activator that has been pointed before as a key player in physiological hypertrophy with its overexpression accounting for increased mitotic figures in exercised hearts (32). Taken together with previous data from the group that showed CITED4 downregulation after TAC and restore after unload, we coupled the unloading model with the cardiac knockout strategy of CITED4, creating a valuable tool to verify the role of CITED4 in the recovery process following pressure overload.

The cardiac specific deletion of CITED4 prior to unload significantly hampered recovery from pressure overload in tamoxifen treated α-MHC-MCM-CITED4$^{f/f}$ mice 3 days after unloading. Only after 7 days did these mice show functional recovery, though not reaching sham levels. Correlating with the delay in functional recovery in these hearts, reversal of fibrosis and stress marker expression was hampered, indicating a possible role of CITED4 herein. Strikingly, regression of LVH occurred in all the unloaded hearts regardless of the treatment and unrelated to the functional outcome. Therefore, we suggest that regression of LVH is a natural outcome when there is relief of pressure overload and does not account solely for enhanced cardiac function.

Furthermore, here we provide clear evidence for mitosis in cardiomyocytes as a necessary step in cardiac function improvement after unloading the pressure overloaded heart. Lack of CITED4 in the heart hinders cell cycle progression to mitosis that is probably reflected on lack of neomyogenesis accounting for a shift towards prominent cell death and fibrosis replacement.

Taken together our data suggests CITED4 is an important mediator of cardiac regeneration which is necessary for a ready recover from pressure overload. Considering that cardiac CITED4 deficient mice showed delayed recovery in response to unloading, it might be hypothesized that by acting as a transcription co-activator it favors the activation of key transcription factors for a fast gene transcription.

Understanding the role of CITED4 on different heart failure models in the future would be beneficial and might open avenues for the use of CITED4 as a

therapeutical target for cardiac pathologies. In order to use CITED4 as a therapeutical target, further research should focus on unravelling specific CITED4 regulators that can be used to stimulate CITED4 activity in the heart. Non-coding RNAs, specifically miRNA and lncRNAs, will probably play a role herein that need confirmation in further research.

Although CITED4 is crucial to trigger a fast recovery from pressure overload in the heart, the effect of exogenous activation of CITED4 should be thoroughly appreciated regarding a possible use in therapy. Importantly, CITED4 has raised interest in cancer field for inhibiting hypoxia-inducible factor-1α transcriptional antagonist activity in cancer cells, which might explain tumor enhancement of hypoxia–inducible factor expression and leading to a more aggressive cancer phenotype (120). Further research on CITED4 binding partners should be performed to enable prevention from undesired cancer related outcomes.

Overall our research points CITED4 has an important key regulator of mitosis in the recovery from pressure overload that contributes considerably for a fast healing process. Although promising as a possible therapeutical target, further research is required to ensure safety of CITED4 stimulation in the Human heart.

VI. References

VI. References

1. Yancy, C. W., Jessup, M., Bozkurt, B., Butler, J., Casey, D. E., Drazner, M. H., Fonarow, G. C., Geraci, S. A., Horwich, T., Januzzi, J. L., Johnson, M. R., Kasper, E. K., Levy, W. C., Masoudi, F. A., McBride, P. E., McMurray, J. J. V, Mitchell, J. E., Peterson, P. N., Riegel, B., Sam, F., Stevenson, L. W., Tang, W. H. W., Tsai, E. J., and Wilkoff, B. L. (2013) 2013 ACCF/AHA guideline for the management of heart failure: a report of the American College of Cardiology Foundation/American Heart Association Task Force on practice guidelines. *Circulation*. **128**, e240–327

2. Kehat, I., and Molkentin, J. D. (2010) Molecular pathways underlying cardiac remodeling during pathophysiological stimulation. *Circulation*. **122**, 2727–35

3. Fedak, P. W. M., Verma, S., Weisel, R. D., and Li, R.-K. (2005) Cardiac remodeling and failure: from molecules to man (Part I). *Cardiovasc. Pathol.* **14**, 1–11

4. Finsterer, J., and Cripe, L. (2014) Treatment of dystrophin cardiomyopathies. *Nat. Rev. Cardiol.* **11**, 168–79

5. Trivedi, C. M., and Epstein, J. A. (2011) Heart-healthy hypertrophy. *Cell Metab.* **13**, 3–4

6. Weeks, K. L., and McMullen, J. R. (2011) The athlete's heart vs. the failing heart: can signaling explain the two distinct outcomes? *Physiology (Bethesda).* **26**, 97–105

7. Dorn, G. W. (2007) The fuzzy logic of physiological cardiac hypertrophy. *Hypertension*. **49**, 962–70

8. Molkentin, J. D. (2004) Calcineurin-NFAT signaling regulates the cardiac hypertrophic response in coordination with the MAPKs. *Cardiovasc. Res.* **63**, 467–75

9. Molkentin, J. D. (2000) Calcineurin and beyond: cardiac hypertrophic signaling. *Circ. Res.* **87**, 731–8

10. Frey, N., McKinsey, T. A., and Olson, E. N. (2000) Decoding calcium signals involved in cardiac growth and function. *Nat. Med.* **6**, 1221–7

11. Molkentin, J. D., Lu, J. R., Antos, C. L., Markham, B., Richardson, J., Robbins, J., Grant, S. R., and Olson, E. N. (1998) A calcineurin-dependent transcriptional pathway for cardiac hypertrophy. *Cell*. **93**, 215–28

12. Wilkins, B. J., Dai, Y.-S., Bueno, O. F., Parsons, S. A., Xu, J., Plank, D. M., Jones, F., Kimball, T. R., and Molkentin, J. D. (2004) Calcineurin/NFAT coupling participates in pathological, but not physiological, cardiac hypertrophy. *Circ. Res.* **94**, 110–8

13. Sussman, M. A., Lim, H. W., Gude, N., Taigen, T., Olson, E. N., Robbins, J., Colbert, M. C., Gualberto, A., Wieczorek, D. F., and Molkentin, J. D. (1998) Prevention of cardiac hypertrophy in mice by calcineurin inhibition. *Science*. **281**, 1690–3

14. Rose, B. A., Force, T., and Wang, Y. (2010) Mitogen-activated protein kinase signaling in the heart: angels versus demons in a heart-breaking tale. *Physiol. Rev.* **90**, 1507–46

15. Maillet, M., van Berlo, J. H., and Molkentin, J. D. (2013) Molecular basis of physiological heart growth: fundamental concepts and new players. *Nat. Rev. Mol. Cell Biol.* **14**, 38–48

16. Bernardo, B. C., Weeks, K. L., Pretorius, L., and McMullen, J. R. (2010) Molecular distinction between physiological and pathological cardiac hypertrophy: experimental findings and therapeutic strategies. *Pharmacol. Ther.* **128**, 191–227

17. Doenst, T., Nguyen, T. D., and Abel, E. D. (2013) Cardiac metabolism in heart failure: implications beyond ATP production. *Circ. Res.* **113**, 709–24

18. Camelliti, P., Borg, T. K., and Kohl, P. (2005) Structural and functional characterisation of cardiac fibroblasts. *Cardiovasc. Res.* **65**, 40–51

19. Souders, C. A., Bowers, S. L. K., and Baudino, T. A. (2009) Cardiac fibroblast: the renaissance cell. *Circ. Res.* **105**, 1164–76

20. Kakkar, R., and Lee, R. T. (2010) Intramyocardial fibroblast myocyte communication. *Circ. Res.* **106**, 47–57

21. Willems, I. E., Havenith, M. G., De Mey, J. G., and Daemen, M. J. (1994) The alpha-smooth muscle actin-positive cells in healing human myocardial scars. *Am. J. Pathol.* **145**, 868–75

22. Frangogiannis, N. G., Michael, L. H., and Entman, M. L. (2000) Myofibroblasts in reperfused myocardial infarcts express the embryonic form of smooth muscle myosin heavy chain (SMemb). *Cardiovasc. Res.* **48**, 89–100

23. Chen, W., and Frangogiannis, N. G. (2013) Fibroblasts in post-infarction inflammation and cardiac repair. *Biochim. Biophys. Acta*. **1833**, 945–53

24. Weber, K. T., Sun, Y., Guarda, E., Katwa, L. C., Ratajska, A., Cleutjens, J. P., and Zhou, G. (1995) Myocardial fibrosis in hypertensive heart disease: an overview of potential regulatory mechanisms. *Eur. Heart J.* **16 Suppl C**, 24–8

25. Chiong, M., Wang, Z. V, Pedrozo, Z., Cao, D. J., Troncoso, R., Ibacache, M., Criollo, A., Nemchenko, A., Hill, J. A., and Lavandero, S. (2011) Cardiomyocyte death: mechanisms and translational implications. *Cell Death Dis.* **2**, e244

26. Harvey, P. A., and Leinwand, L. A. (2011) The cell biology of disease: cellular mechanisms of cardiomyopathy. *J. Cell Biol.* **194**, 355–65

27. Diwan, A., and Dorn, G. W. (2007) Decompensation of cardiac hypertrophy: cellular mechanisms and novel therapeutic targets. *Physiology (Bethesda).* **22**, 56–64

28. Waring, C. D., Vicinanza, C., Papalamprou, A., Smith, A. J., Purushothaman, S., Goldspink, D. F., Nadal-Ginard, B., Torella, D., and Ellison, G. M. (2012) The adult

heart responds to increased workload with physiologic hypertrophy, cardiac stem cell activation, and new myocyte formation. *Eur. Heart J.* 10.1093/eurheartj/ehs338

29. Miyamoto, T., Takeishi, Y., Takahashi, H., Shishido, T., Arimoto, T., Tomoike, H., and Kubota, I. (2004) Activation of distinct signal transduction pathways in hypertrophied hearts by pressure and volume overload. *Basic Res. Cardiol.* **99**, 328–37

30. Chaanine, A. H., and Hajjar, R. J. (2011) AKT signalling in the failing heart. *Eur. J. Heart Fail.* **13**, 825–9

31. Waring, C. D., Vicinanza, C., Papalamprou, A., Smith, A. J., Purushothaman, S., Goldspink, D. F., Nadal-Ginard, B., Torella, D., and Ellison, G. M. (2014) The adult heart responds to increased workload with physiologic hypertrophy, cardiac stem cell activation, and new myocyte formation. *Eur. Heart J.* **35**, 2722–31

32. Boström, P., Mann, N., Wu, J., Quintero, P. A., Plovie, E. R., Panáková, D., Gupta, R. K., Xiao, C., MacRae, C. A., Rosenzweig, A., and Spiegelman, B. M. (2010) C/EBPβ controls exercise-induced cardiac growth and protects against pathological cardiac remodeling. *Cell*. **143**, 1072–83

33. Leite, C. F., Lopes, C. S., Alves, A. C., Fuzaro, C. S. C., Silva, M. V., Oliveira, L. F. de, Garcia, L. P., Farnesi, T. S., Cuba, M. B. de, Rocha, L. B., Rodrigues, V., Oliveira, C. J. F. de, and Dias da Silva, V. J. (2015) Endogenous resident c-Kit cardiac stem cells increase in mice with an exercise-induced, physiologically hypertrophied heart. *Stem Cell Res.* **15**, 151–164

34. Beltrami, A. P., Urbanek, K., Kajstura, J., Yan, S. M., Finato, N., Bussani, R., Nadal-Ginard, B., Silvestri, F., Leri, A., Beltrami, C. A., and Anversa, P. (2001) Evidence that human cardiac myocytes divide after myocardial infarction. *N. Engl. J. Med.* **344**, 1750–7

35. Meckert, P. C., Rivello, H. G., Vigliano, C., González, P., Favaloro, R., and Laguens, R. (2005) Endomitosis and polyploidization of myocardial cells in the periphery of human acute myocardial infarction. *Cardiovasc. Res.* **67**, 116–23

36. Li, Y., Hu, S., Ma, G., Yao, Y., Yan, G., Chen, J., Li, Y., and Zhang, Z. (2013) Acute myocardial infarction induced functional cardiomyocytes to re-enter the cell cycle. *Am. J. Transl. Res.* **5**, 327–35

37. Ahuja, P., Sdek, P., and MacLellan, W. R. (2007) Cardiac myocyte cell cycle control in development, disease, and regeneration. *Physiol. Rev.* **87**, 521–44

38. Kajstura, J., Cheng, W., Reiss, K., and Anversa, P. (1994) The IGF-1-IGF-1 receptor system modulates myocyte proliferation but not myocyte cellular hypertrophy in vitro. *Exp. Cell Res.* **215**, 273–83

39. Reiss, K., Cheng, W., Ferber, A., Kajstura, J., Li, P., Li, B., Olivetti, G., Homcy, C. J., Baserga, R., and Anversa, P. (1996) Overexpression of insulin-like growth factor-1 in the heart is coupled with myocyte proliferation in transgenic mice. *Proc. Natl. Acad. Sci. U. S. A.* **93**, 8630–5

40. Condorelli, G., Drusco, A., Stassi, G., Bellacosa, A., Roncarati, R., Iaccarino, G., Russo, M. A., Gu, Y., Dalton, N., Chung, C., Latronico, M. V. G., Napoli, C., Sadoshima, J., Croce, C. M., and Ross, J. (2002) Akt induces enhanced myocardial contractility and cell size in vivo in transgenic mice. *Proc. Natl. Acad. Sci. U. S. A.* **99**, 12333–8

41. Gude, N., Muraski, J., Rubio, M., Kajstura, J., Schaefer, E., Anversa, P., and Sussman, M. A. (2006) Akt promotes increased cardiomyocyte cycling and expansion of the cardiac progenitor cell population. *Circ. Res.* **99**, 381–8

42. Torella, D., Rota, M., Nurzynska, D., Musso, E., Monsen, A., Shiraishi, I., Zias, E., Walsh, K., Rosenzweig, A., Sussman, M. A., Urbanek, K., Nadal-Ginard, B., Kajstura, J., Anversa, P., and Leri, A. (2004) Cardiac stem cell and myocyte aging, heart failure, and insulin-like growth factor-1 overexpression. *Circ. Res.* **94**, 514–24

43. Packer, M., Fowler, M. B., Roecker, E. B., Coats, A. J. S., Katus, H. A., Krum, H., Mohacsi, P., Rouleau, J. L., Tendera, M., Staiger, C., Holcslaw, T. L., Amann-Zalan, I., and DeMets, D. L. (2002) Effect of carvedilol on the morbidity of patients with severe chronic heart failure: results of the carvedilol prospective randomized cumulative survival (COPERNICUS) study. *Circulation*. **106**, 2194–9

44. Bristow, M. R. (2000) beta-adrenergic receptor blockade in chronic heart failure. *Circulation*. **101**, 558–69

45. Demers, C., Mody, A., Teo, K. K., and McKelvie, R. S. (2005) ACE inhibitors in heart failure: what more do we need to know? *Am. J. Cardiovasc. Drugs*. **5**, 351–9

46. Garg, R., and Yusuf, S. (1995) Overview of randomized trials of angiotensin-converting enzyme inhibitors on mortality and morbidity in patients with heart failure. Collaborative Group on ACE Inhibitor Trials. *JAMA*. **273**, 1450–6

47. Carabello, B. A. (2011) Transcatheter aortic-valve implantation for aortic stenosis in patients who cannot undergo surgery. *Curr. Cardiol. Rep.* **13**, 173–4

48. Rogers, J. H., and Bolling, S. F. (2012) What to do with functional mitral regurgitation: what do we really know and how can we find out? *Eur. J. Cardiothorac. Surg.* **42**, 915–7

49. Phillips, H. R., O'Connor, C. M., and Rogers, J. (2007) Revascularization for heart failure. *Am. Heart J.* **153**, 65–73

50. Beltrami, A. P., Barlucchi, L., Torella, D., Baker, M., Limana, F., Chimenti, S., Kasahara, H., Rota, M., Musso, E., Urbanek, K., Leri, A., Kajstura, J., Nadal-Ginard, B., and Anversa, P. (2003) Adult cardiac stem cells are multipotent and support myocardial regeneration. *Cell*. **114**, 763–76

51. Oyama, T., Nagai, T., Wada, H., Naito, A. T., Matsuura, K., Iwanaga, K., Takahashi, T., Goto, M., Mikami, Y., Yasuda, N., Akazawa, H., Uezumi, A., Takeda, S., and Komuro, I. (2007) Cardiac side population cells have a potential to migrate and differentiate into cardiomyocytes in vitro and in vivo. *J. Cell Biol.* **176**, 329–41

52. Matsuura, K., Nagai, T., Nishigaki, N., Oyama, T., Nishi, J., Wada, H., Sano, M., Toko, H., Akazawa, H., Sato, T., Nakaya, H., Kasanuki, H., and Komuro, I. (2004) Adult cardiac Sca-1-positive cells differentiate into beating cardiomyocytes. *J. Biol. Chem.* **279**, 11384–91

53. Cai, C.-L., Liang, X., Shi, Y., Chu, P.-H., Pfaff, S. L., Chen, J., and Evans, S. (2003) Isl1 identifies a cardiac progenitor population that proliferates prior to differentiation and contributes a majority of cells to the heart. *Dev. Cell*. **5**, 877–89

54. Laugwitz, K.-L., Moretti, A., Lam, J., Gruber, P., Chen, Y., Woodard, S., Lin, L.-Z., Cai, C.-L., Lu, M. M., Reth, M., Platoshyn, O., Yuan, J. X.-J., Evans, S., and Chien, K. R. (2005) Postnatal isl1+ cardioblasts enter fully differentiated cardiomyocyte lineages. *Nature*. **433**, 647–53

55. Assmus, B., Rolf, A., Erbs, S., Elsässer, A., Haberbosch, W., Hambrecht, R., Tillmanns, H., Yu, J., Corti, R., Mathey, D. G., Hamm, C. W., Süselbeck, T., Tonn, T., Dimmeler, S., Dill, T., Zeiher, A. M., and Schächinger, V. (2010) Clinical outcome 2 years after intracoronary administration of bone marrow-derived progenitor cells in acute myocardial infarction. *Circ. Heart Fail.* **3**, 89–96

56. Marbán, E., and Malliaras, K. (2012) Mixed results for bone marrow–derived cell therapy for ischemic heart disease. *JAMA*. **308**, 2405–6

57. Traverse, J. H., Henry, T. D., Pepine, C. J., Willerson, J. T., Zhao, D. X. M., Ellis, S. G., Forder, J. R., Anderson, R. D., Hatzopoulos, A. K., Penn, M. S., Perin, E. C., Chambers, J., Baran, K. W., Raveendran, G., Lambert, C., Lerman, A., Simon, D. I., Vaughan, D. E., Lai, D., Gee, A. P., Taylor, D. A., Cogle, C. R., Thomas, J. D., Olson, R. E., Bowman, S., Francescon, J., Geither, C., Handberg, E., Kappenman, C., Westbrook, L., Piller, L. B., Simpson, L. M., Baraniuk, S., Loghin, C., Aguilar, D., Richman, S., Zierold, C., Spoon, D. B., Bettencourt, J., Sayre, S. L., Vojvodic, R. W., Skarlatos, S. I., Gordon, D. J., Ebert, R. F., Kwak, M., Moyé, L. A., and Simari, R. D. (2012) Effect of the use and timing of bone marrow mononuclear cell delivery on left ventricular function after acute myocardial infarction: the TIME randomized trial. *JAMA*. **308**, 2380–9

58. Hare, J. M., Fishman, J. E., Gerstenblith, G., DiFede Velazquez, D. L., Zambrano, J. P., Suncion, V. Y., Tracy, M., Ghersin, E., Johnston, P. V, Brinker, J. A., Breton, E., Davis-Sproul, J., Schulman, I. H., Byrnes, J., Mendizabal, A. M., Lowery, M. H., Rouy, D., Altman, P., Wong Po Foo, C., Ruiz, P., Amador, A., Da Silva, J., McNiece, I. K., Heldman, A. W., George, R., and Lardo, A. (2012) Comparison of allogeneic vs autologous bone marrow–derived mesenchymal stem cells delivered by transendocardial injection in patients with ischemic cardiomyopathy: the POSEIDON randomized trial. *JAMA*. **308**, 2369–79

59. Menasché, P., Alfieri, O., Janssens, S., McKenna, W., Reichenspurner, H., Trinquart, L., Vilquin, J.-T., Marolleau, J.-P., Seymour, B., Larghero, J., Lake, S., Chatellier, G., Solomon, S., Desnos, M., and Hagège, A. A. (2008) The Myoblast Autologous Grafting in Ischemic Cardiomyopathy (MAGIC) trial: first randomized placebo-controlled study of myoblast transplantation. *Circulation*. **117**, 1189–200

60. Rubart, M., Soonpaa, M. H., Nakajima, H., and Field, L. J. (2004) Spontaneous and evoked intracellular calcium transients in donor-derived myocytes following intracardiac myoblast transplantation. *J. Clin. Invest.* **114**, 775–83

61. Choi, W.-Y., and Poss, K. D. (2012) Cardiac regeneration. *Curr. Top. Dev. Biol.* **100**, 319–44

62. Garbern, J. C., and Lee, R. T. (2013) Cardiac stem cell therapy and the promise of heart regeneration. *Cell Stem Cell*. **12**, 689–98

63. Van Berlo, J. H., Kanisicak, O., Maillet, M., Vagnozzi, R. J., Karch, J., Lin, S.-C. J., Middleton, R. C., Marbán, E., and Molkentin, J. D. (2014) c-kit+ cells minimally contribute cardiomyocytes to the heart. *Nature*. **509**, 337–41

64. Pasumarthi, K. B. S. (2002) Cardiomyocyte Cell Cycle Regulation. *Circ. Res.* **90**, 1044–1054

65. Kikuchi, K., and Poss, K. D. (2012) Cardiac regenerative capacity and mechanisms. *Annu. Rev. Cell Dev. Biol.* **28**, 719–41

66. Segers, V. F. M., and Lee, R. T. (2008) Stem-cell therapy for cardiac disease. *Nature*. **451**, 937–42

67. Levin, H. R., Oz, M. C., Chen, J. M., Packer, M., Rose, E. A., and Burkhoff, D. (1995) Reversal of chronic ventricular dilation in patients with end-stage cardiomyopathy by prolonged mechanical unloading. *Circulation*. **91**, 2717–20

68. Frazier, O. H., Benedict, C. R., Radovancevic, B., Bick, R. J., Capek, P., Springer, W. E., Macris, M. P., Delgado, R., and Buja, L. M. (1996) Improved left ventricular function after chronic left ventricular unloading. *Ann. Thorac. Surg.* **62**, 675–81; discussion 681–2

69. Depre, C., Shipley, G. L., Chen, W., Han, Q., Doenst, T., Moore, M. L., Stepkowski, S., Davies, P. J., and Taegtmeyer, H. (1998) Unloaded heart in vivo replicates fetal gene expression of cardiac hypertrophy. *Nat. Med.* **4**, 1269–75

70. Koshman, Y. E., Patel, N., Chu, M., Iyengar, R., Kim, T., Ersahin, C., Lewis, W., Heroux, A., and Samarel, A. M. (2013) Regulation of connective tissue growth factor gene expression and fibrosis in human heart failure. *J. Card. Fail.* **19**, 283–94

71. Rivello, H. G., Meckert, P. C., Vigliano, C., Favaloro, R., and Laguens, R. P. (2001) Cardiac myocyte nuclear size and ploidy status decrease after mechanical support. *Cardiovasc. Pathol.* **10**, 53–7

72. Wohlschlaeger, J., Levkau, B., Brockhoff, G., Schmitz, K. J., von Winterfeld, M., Takeda, A., Takeda, N., Stypmann, J., Vahlhaus, C., Schmid, C., Pomjanski, N., Böcking, A., and Baba, H. A. (2010) Hemodynamic support by left ventricular assist devices reduces cardiomyocyte DNA content in the failing human heart. *Circulation*. **121**, 989–96

73. Givertz, M. M. (2011) Cardiology patient pages: ventricular assist devices: important information for patients and families. *Circulation*. **124**, e305–11

74. Porrello, E. R., Widdop, R. E., and Delbridge, L. M. D. (2008) Early origins of cardiac hypertrophy: does cardiomyocyte attrition programme for pathological "catch-up" growth of the heart? *Clin. Exp. Pharmacol. Physiol.* **35**, 1358–64

75. Li, F., Wang, X., Capasso, J. M., and Gerdes, A. M. (1996) Rapid transition of cardiac myocytes from hyperplasia to hypertrophy during postnatal development. *J. Mol. Cell. Cardiol.* **28**, 1737–46

76. Laflamme, M. A., and Murry, C. E. (2011) Heart regeneration. *Nature*. **473**, 326–35

77. Sherr, C. J. (1994) G1 phase progression: cycling on cue. *Cell*. **79**, 551–5

78. Cobrinik, D. (2005) Pocket proteins and cell cycle control. *Oncogene*. **24**, 2796–809

79. Chiu, J., and Dawes, I. W. (2012) Redox control of cell proliferation. *Trends Cell Biol.* **22**, 592–601

80. Brooks, G., Poolman, R. A., McGill, C. J., and Li, J. M. (1997) Expression and activities of cyclins and cyclin-dependent kinases in developing rat ventricular myocytes. *J. Mol. Cell. Cardiol.* **29**, 2261–71

81. Kang, M. J., and Koh, G. Y. (1997) Differential and dramatic changes of cyclin-dependent kinase activities in cardiomyocytes during the neonatal period. *J. Mol. Cell. Cardiol.* **29**, 1767–77

82. Sherr, C. J., and Roberts, J. M. (2004) Living with or without cyclins and cyclin-dependent kinases. *Genes Dev.* **18**, 2699–711

83. Kozar, K., Ciemerych, M. A., Rebel, V. I., Shigematsu, H., Zagozdzon, A., Sicinska, E., Geng, Y., Yu, Q., Bhattacharya, S., Bronson, R. T., Akashi, K., and Sicinski, P. (2004) Mouse development and cell proliferation in the absence of D-cyclins. *Cell*. **118**, 477–91

84. Pasumarthi, K. B. S., Nakajima, H., Nakajima, H. O., Soonpaa, M. H., and Field, L. J. (2005) Targeted expression of cyclin D2 results in cardiomyocyte DNA synthesis and infarct regression in transgenic mice. *Circ. Res.* **96**, 110–8

85. Berthet, C., Klarmann, K. D., Hilton, M. B., Suh, H. C., Keller, J. R., Kiyokawa, H., and Kaldis, P. (2006) Combined loss of Cdk2 and Cdk4 results in embryonic lethality and Rb hypophosphorylation. *Dev. Cell*. **10**, 563–73

86. Jiang, Z., Zacksenhaus, E., Gallie, B. L., and Phillips, R. A. (1997) The retinoblastoma gene family is differentially expressed during embryogenesis. *Oncogene*. **14**, 1789–97

87. Clarke, A. R., Maandag, E. R., van Roon, M., van der Lugt, N. M., van der Valk, M., Hooper, M. L., Berns, A., and te Riele, H. (1992) Requirement for a functional Rb-1 gene in murine development. *Nature*. **359**, 328–30

88. MacLellan, W. R., Garcia, A., Oh, H., Frenkel, P., Jordan, M. C., Roos, K. P., and Schneider, M. D. (2005) Overlapping roles of pocket proteins in the myocardium are unmasked by germ line deletion of p130 plus heart-specific deletion of Rb. *Mol. Cell. Biol.* **25**, 2486–97

89. Jackson, T., Allard, M. F., Sreenan, C. M., Doss, L. K., Bishop, S. P., and Swain, J. L. (1990) The c-myc proto-oncogene regulates cardiac development in transgenic mice. *Mol. Cell. Biol.* **10**, 3709–16

90. Davis, A. C., Wims, M., Spotts, G. D., Hann, S. R., and Bradley, A. (1993) A null c-myc mutation causes lethality before 10.5 days of gestation in homozygotes and reduced fertility in heterozygous female mice. *Genes Dev.* **7**, 671–82

91. Felsher, D. W., Zetterberg, A., Zhu, J., Tlsty, T., and Bishop, J. M. (2000) Overexpression of MYC causes p53-dependent G2 arrest of normal fibroblasts. *Proc. Natl. Acad. Sci. U. S. A.* **97**, 10544–8

92. Koshiji, M., Kageyama, Y., Pete, E. A., Horikawa, I., Barrett, J. C., and Huang, L. E. (2004) HIF-1alpha induces cell cycle arrest by functionally counteracting Myc. *EMBO J.* **23**, 1949–56

93. Iyer, N. V, Kotch, L. E., Agani, F., Leung, S. W., Laughner, E., Wenger, R. H., Gassmann, M., Gearhart, J. D., Lawler, A. M., Yu, A. Y., and Semenza, G. L. (1998) Cellular and developmental control of O2 homeostasis by hypoxia-inducible factor 1 alpha. *Genes Dev.* **12**, 149–62

94. Krishnan, J., Suter, M., Windak, R., Krebs, T., Felley, A., Montessuit, C., Tokarska-Schlattner, M., Aasum, E., Bogdanova, A., Perriard, E., Perriard, J.-C., Larsen, T., Pedrazzini, T., and Krek, W. (2009) Activation of a HIF1alpha-PPARgamma axis underlies the integration of glycolytic and lipid anabolic pathways in pathologic cardiac hypertrophy. *Cell Metab.* **9**, 512–24

95. Barr, F. A., and Gruneberg, U. (2007) Cytokinesis: placing and making the final cut. *Cell*. **131**, 847–60

96. Li, F., Wang, X., Bunger, P. C., and Gerdes, A. M. (1997) Formation of binucleated cardiac myocytes in rat heart: I. Role of actin-myosin contractile ring. *J. Mol. Cell. Cardiol.* **29**, 1541–51

97. Kajstura, J., Leri, A., Finato, N., Di Loreto, C., Beltrami, C. A., and Anversa, P. (1998) Myocyte proliferation in end-stage cardiac failure in humans. *Proc. Natl. Acad. Sci. U. S. A.* **95**, 8801–5

98. Bragança, J., Swingler, T., Marques, F. I. R., Jones, T., Eloranta, J. J., Hurst, H. C., Shioda, T., and Bhattacharya, S. (2002) Human CREB-binding protein/p300-interacting transactivator with ED-rich tail (CITED) 4, a new member of the CITED family, functions as a co-activator for transcription factor AP-2. *J. Biol. Chem.* **277**, 8559–65

99. Ryall, K. A., Bezzerides, V. J., Rosenzweig, A., and Saucerman, J. J. (2014) Phenotypic screen quantifying differential regulation of cardiac myocyte hypertrophy identifies CITED4 regulation of myocyte elongation. *J. Mol. Cell. Cardiol.* **72C**, 74–84

100. Sohal, D. S., Nghiem, M., Crackower, M. A., Witt, S. A., Kimball, T. R., Tymitz, K. M., Penninger, J. M., and Molkentin, J. D. (2001) Temporally regulated and tissue-specific gene manipulations in the adult and embryonic heart using a tamoxifen-inducible Cre protein. *Circ. Res.* **89**, 20–5

101. Bourajjaj, M., Armand, A.-S., da Costa Martins, P. A., Weijts, B., van der Nagel, R., Heeneman, S., Wehrens, X. H., and De Windt, L. J. (2008) NFATc2 is a necessary mediator of calcineurin-dependent cardiac hypertrophy and heart failure. *J. Biol. Chem.* **283**, 22295–303

102. Rockman, H. A., Ross, R. S., Harris, A. N., Knowlton, K. U., Steinhelper, M. E., Field, L. J., Ross, J., and Chien, K. R. (1991) Segregation of atrial-specific and inducible expression of an atrial natriuretic factor transgene in an in vivo murine model of cardiac hypertrophy. *Proc. Natl. Acad. Sci. U. S. A.* **88**, 8277–81

103. Verma, S. K., Krishnamurthy, P., and Kishore, R. (2014) *Manual of Research Techniques in Cardiovascular Medicine*, John Wiley & Sons, Ltd, Oxford, UK, 10.1002/9781118495148

104. deAlmeida, A. C., van Oort, R. J., and Wehrens, X. H. T. (2010) Transverse aortic constriction in mice. *J. Vis. Exp.* 10.3791/1729

105. Wahlquist, C., Jeong, D., Rojas-Muñoz, A., Kho, C., Lee, A., Mitsuyama, S., van Mil, A., Park, W. J., Sluijter, J. P. G., Doevendans, P. A. F., Hajjar, R. J., and Mercola, M. (2014) Inhibition of miR-25 improves cardiac contractility in the failing heart. *Nature*. **508**, 531–5

106. Van den Bosch, B. J. C., Lindsey, P. J., van den Burg, C. M. M., van der Vlies, S. A., Lips, D. J., van der Vusse, G. J., Ayoubi, T. A., Doevendans, P. A., and Smeets, H. J. M. (2006) Early and transient gene expression changes in pressure overload-induced cardiac hypertrophy in mice. *Genomics*. **88**, 480–8

107. Moore-Morris, T., Guimarães-Camboa, N., Banerjee, I., Zambon, A. C., Kisseleva, T., Velayoudon, A., Stallcup, W. B., Gu, Y., Dalton, N. D., Cedenilla, M., Gomez-Amaro, R., Zhou, B., Brenner, D. A., Peterson, K. L., Chen, J., and Evans, S. M. (2014) Resident fibroblast lineages mediate pressure overload-induced cardiac fibrosis. *J. Clin. Invest.* **124**, 2921–34

108. Fiedler, L., Jenkins, M., Maifoshie, E., Harada, M., Stuckey, D., Song, W., Sampson, R., Harding, S., and Schneider, M. (2014) MAP4K4 mediates cardiomyocyte cell death and potentiates a heart failure phentotype. *Heart*. **100**, A20–A20

109. Gandhi, M. S., Kamalov, G., Shahbaz, A. U., Bhattacharya, S. K., Ahokas, R. A., Sun, Y., Gerling, I. C., and Weber, K. T. (2011) Cellular and molecular pathways to myocardial necrosis and replacement fibrosis. *Heart Fail. Rev.* **16**, 23–34

110. Yuasa, S., Fukuda, K., Tomita, Y., Fujita, J., Ieda, M., Tahara, S., Itabashi, Y., Yagi, T., Kawaguchi, H., Hisaka, Y., and Ogawa, S. (2004) Cardiomyocytes undergo cells division following myocardial infarction is a spatially and temporally restricted event in rats. *Mol. Cell. Biochem.* **259**, 177–81

111. Hou, J., and Kang, Y. J. (2012) Regression of pathological cardiac hypertrophy: signaling pathways and therapeutic targets. *Pharmacol. Ther.* **135**, 337–54

112. Rodrigue-Way, A., Burkhoff, D., Geesaman, B. J., Golden, S., Xu, J., Pollman, M. J., Donoghue, M., Jeyaseelan, R., Houser, S., Breitbart, R. E., Marks, A., and Acton, S. (2005) Sarcomeric genes involved in reverse remodeling of the heart during left ventricular assist device support. *J. Heart Lung Transplant.* **24**, 73–80

113. Dobaczewski, M., Chen, W., and Frangogiannis, N. G. (2011) Transforming growth factor (TGF)-β signaling in cardiac remodeling. *J. Mol. Cell. Cardiol.* **51**, 600–6

114. Bjørnstad, J. L., Sjaastad, I., Nygård, S., Hasic, A., Ahmed, M. S., Attramadal, H., Finsen, A. V., Christensen, G., and Tønnessen, T. (2011) Collagen isoform shift during the early phase of reverse left ventricular remodelling after relief of pressure overload. *Eur. Heart J.* **32**, 236–45

115. Li, R.-C., Tao, J., Guo, Y.-B., Wu, H.-D., Liu, R.-F., Bai, Y., Lv, Z.-Z., Luo, G.-Z., Li, L.-L., Wang, M., Yang, H.-Q., Gao, W., Han, Q.-D., Zhang, Y.-Y., Wang, X.-J., Xu, M., and Wang, S.-Q. (2013) In Vivo Suppression of MicroRNA-24 Prevents the Transition Toward Decompensated Hypertrophy in Aortic-Constricted Mice. *Circ. Res.* **112**, 601–605

116. Liu, X., Xiao, J., Zhu, H., Wei, X., Platt, C., Damilano, F., Xiao, C., Bezzerides, V., Boström, P., Che, L., Zhang, C., Spiegelman, B. M., and Rosenzweig, A. (2015) miR-222 Is Necessary for Exercise-Induced Cardiac Growth and Protects against Pathological Cardiac Remodeling. *Cell Metab.* **21**, 584–595

117. Yang, K.-C., Yamada, K. A., Patel, A. Y., Topkara, V. K., George, I., Cheema, F. H., Ewald, G. A., Mann, D. L., and Nerbonne, J. M. (2014) Deep RNA sequencing reveals dynamic regulation of myocardial noncoding RNAs in failing human heart and remodeling with mechanical circulatory support. *Circulation*. **129**, 1009–21

118. Von Harsdorf, R., Hauck, L., Mehrhof, F., Wegenka, U., Cardoso, M. C., and Dietz, R. (1999) E2F-1 overexpression in cardiomyocytes induces downregulation of p21CIP1 and p27KIP1 and release of active cyclin-dependent kinases in the presence of insulin-like growth factor I. *Circ. Res.* **85**, 128–36

119. Reiss, K., Cheng, W., Pierzchalski, P., Kodali, S., Li, B., Wang, S., Liu, Y., and Anversa, P. (1997) Insulin-like growth factor-1 receptor and its ligand regulate the reentry of adult ventricular myocytes into the cell cycle. *Exp. Cell Res.* **235**, 198–209

120. Fox, S. B., Bragança, J., Turley, H., Campo, L., Han, C., Gatter, K. C., Bhattacharya, S., and Harris, A. L. (2004) CITED4 inhibits hypoxia-activated transcription in cancer cells, and its cytoplasmic location in breast cancer is associated with elevated expression of tumor cell hypoxia-inducible factor 1alpha. *Cancer Res.* **64**, 6075–81

VII. Supplements

VII. Supplements

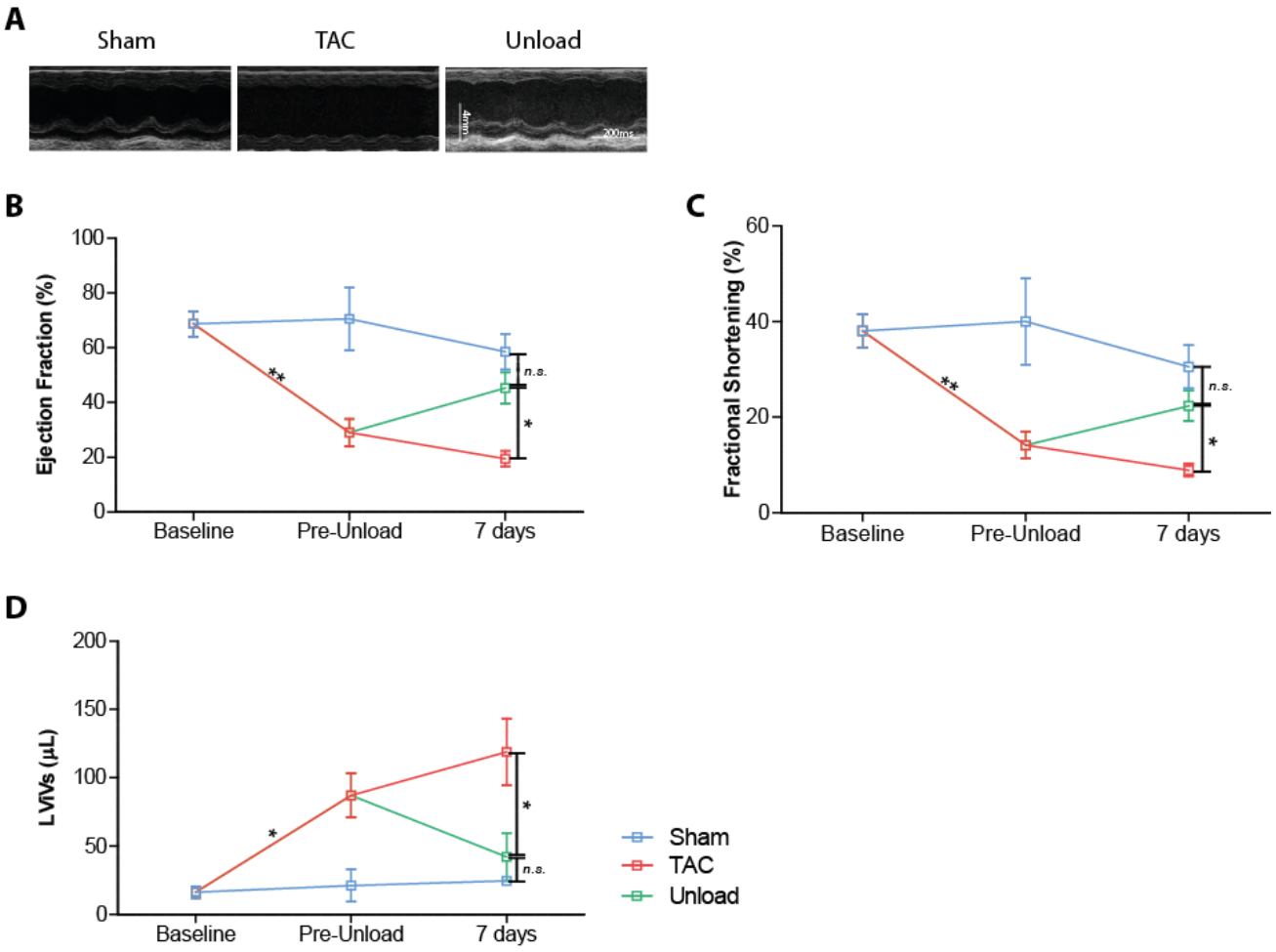

FIGURE 11 | Aortic constriction induces decrease of heart function that is fully restored upon unloading in CITED4$^{f/f}$ mice. *A*. representative M-mode images of tamoxifen treated CITED4$^{f/f}$ mice 7 days after the unloading time-point, indicating increased LV internal dimensions after pressure overload that are reversed upon unloading. *Time scale* and *size* indication are depicted in the M-mode images. *B-D*. Graphical representation of (*B*.) fractional shortening (FS), (*C*.) ejection fraction (EF) and (*D*.) LV internal volume at systole (LViVs), indicating decreased function and geometrical deterioration after TAC that is reversed upon unloading (n=3 – 6/ group). *Error bars* are represented as Mean ± SEM; *n.s.*, not significant; * p<0,05; ** *p*<0,01.